VOLUME 4

MIT Quantum Science and Engineering Consortium

QSEC Quarterly

Spring 2022

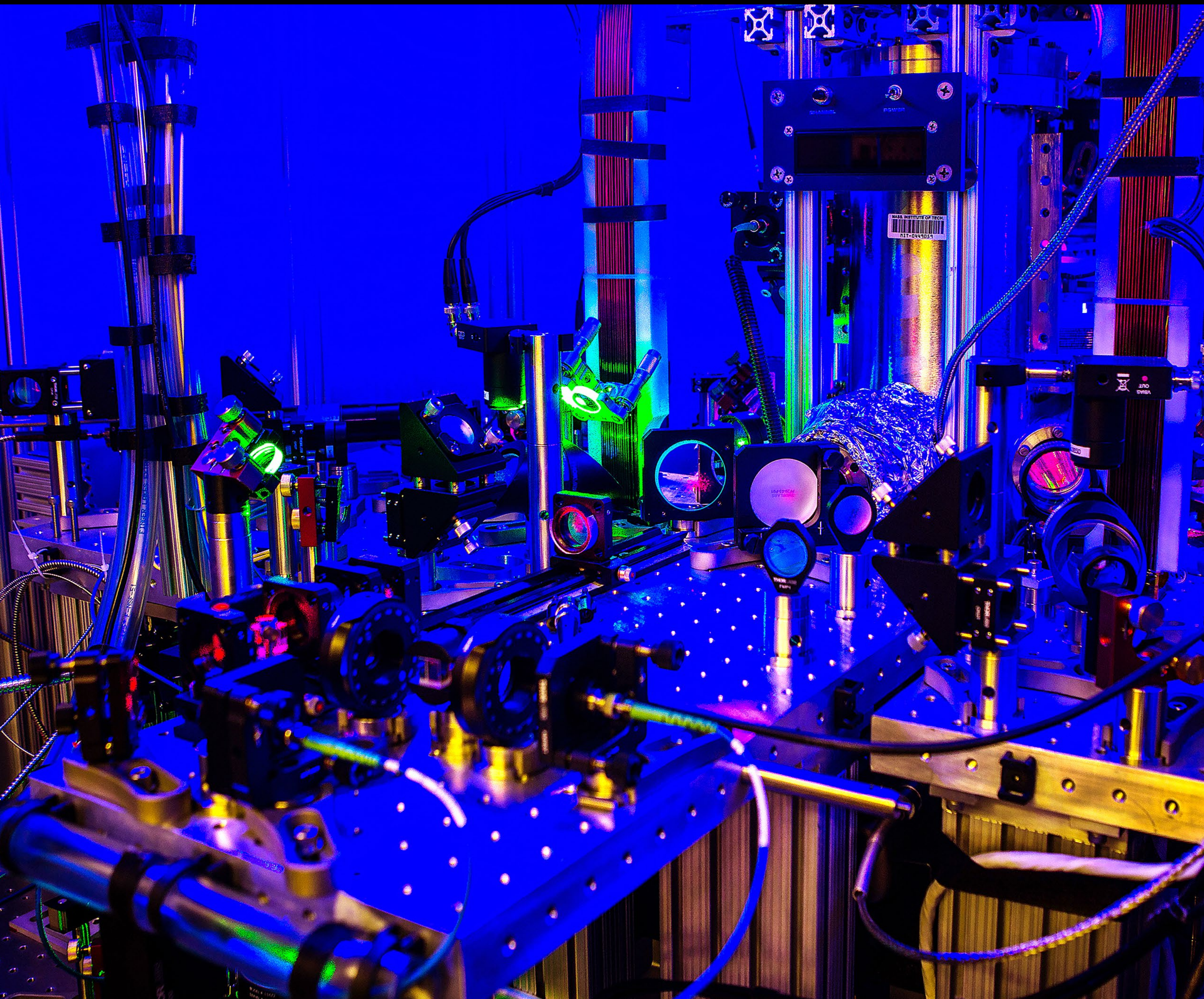

Contents

MIT-CQE Mission

MIT's Center for Quantum Engineering is dedicated to the academic pursuit and practice of science and engineering to accelerate the practical application of quantum technologies for the betterment of humankind.

FROM THE DIRECTOR

It is our pleasure to present the Spring 2022 edition of the Quantum Science and Engineering Consortium (QSEC) newsletter.

The spring term concluded in late May, and the summer is now well underway at MIT. With it brings a number of exciting developments for the MIT quantum community.

Our QSEC membership group is growing! We extend a warm welcome to our new members:

- Sustaining members: Airbus, Equinor, and JPMorgan Chase & Co.,
- Start-up members: QuEra Computing and Turing,
- Non-profit member: Second Foundation.

In addition, we are pleased to welcome several faculty to the Center for Quantum Engineering:

- Prof. Michael Carbin, EECS – quantum programming languages
- Prof. Song Han, EECS – quantum and quantum-inspired algorithms
- Prof. Farnaz Niroui, EECS – quantum control and integration technologies

The summer is a time for both focused research and well-earned downtime with family and friends.

DIRECTOR
MIT Center for Quantum Engineering (CQE)

PROFESSOR
of Electrical Engineering and Computer Science and of Physics

LINCOLN LABORATORY FELLOW

Wishing you all a productive and prosperous summer 2022!

William D. Oliver

William D. Oliver
william.oliver@mit.edu

CQE PI FEATURE

Where Physics Meets Computer Science

ANAND NATARAJAN
Assistant Professor, Electrical Engineering and Computer Science

My research is on quantum complexity theory: the study of the computational power and limitations of quantum computers, and more generally models of computation that use quantum mechanics. More specifically, much of my research focuses on the complexity of proofs: how hard is it, not to solve a computational problem, but to certify to a computationally limited verifier that a hard problem has been solved correctly. In the quantum world, proofs give us a fascinating new lens to study entanglement, which is one of the most characteristic phenomena of quantum mechanics. Quantum proof systems may also be useful in practice, in the likely case that quantum computers become available over the cloud: users will want to certify that their computations were performed correctly by the machine in the cloud. There is also a rich theory around proof complexity and related topics (such as constraint satisfaction problems) in classical computer science, and much of my research focuses on areas in which the quantum picture is strikingly different from the classical one.

My current projects span a few different directions. With Tina Zhang (a student at MIT), 3Honghao Fu (a postdoc at MIT), and John Wright (faculty at UC Berkeley), I have been studying several questions on the complexity of nonlocal games, motivated by my postdoctoral work with John and others on the complexity class MIP*. That work used computational complexity theory to construct an interactive protocol---a game, or a Bell test in the terminology of physics---that could distinguish between two models of quantum mechanics that had hitherto been considered to be equivalent. We are exploring whether the analysis of our protocol can be drastically simplified using tools from classical computer science, and whether the protocol itself can be cast in an especially simple form known as a linear constraint system game. If we succeed, our results could be useful to mathematicians working in group theory, and the t heory of operator algebras.

Other directions I am studying, together with Sunny He and Sujit Rao (students at MIT) and Chinmay Nirkhe (a student at UC Berkeley) are focused on quantum proof states that can be efficiently verified by quantum computers. We are interested in understanding the difficulty of physically preparing such proof states, even given access to substantial classical "hints" (such as the ability to query a computationally powerful oracle). We are also working towards understanding when quantum proof states give an advantage over classical proofs (the QMA vs QCMA problem, in complexity jargon), as well as connections between quantum proofs and quantum error correcting codes (problems related to the quantum PCP conjecture).

I first got interested in quantum information as an undergraduate studying physics at Stanford. I had an independent interest in the theory of computation, and reading some lecture notes and blog posts by Scott Aaronson (formerly at MIT, now at UT Austin) convinced me that quantum computing was a field that combined the best parts of fundamental physics and theoretical computer science. Scott's writings laid out the case that building a quantum computer is not just about breaking codes or designing catalysts, but addresses the fundamental scientific question of what can be efficiently computed in our physical universe. I started my PhD in 2013 with Aram Harrow at the Center for Theoretical Physics at MIT, and over the last 9 years I've been thrilled to watch the rapid progress that quantum computing has made, and the surprising ways in which it has intersected other fields. One of my favorite things about our field is that, since it is so young, students can quickly reach the research frontier and start participating as full-fledged members of the community: indeed, many breakthroughs of the last few years were made by graduate students. I personally greatly enjoy working with my collaborators at all levels of seniority and I deeply value the friendships I have made along the way, which have helped to keep me going even during research setbacks.

CQE STUDENT FEATURE

MIT Theory of Computing: Sujit Rao

Research group name: Theory of Computing

Research Advisor: Anand Natarajan

Hometown, Country: Columbus, Ohio, USA

Academic History Prior to coming to MIT: BA in Mathematics and Computer Science at Cornell

What brought you to MIT? MIT has many faculty and students working in several related areas, including applied math, theoretical computer science, quantum information, and others. Having people with such a wide range of interests is becoming more important as research becomes more and more interdisciplinary.

What interests you the most about your research? Quantum computing still needs more experimental work to be realized in a lab, so sometimes it can be unclear what the direct impact of theoretical research is. But it can still give fundamental insights on topics such as entanglement, computational complexity, and classical algorithms and machine learning, and with any luck could help to build an experimental quantum computer. The most interesting theoretical results state fundamental limits on physical processes in very general settings and with minimal assumptions, which would give insights on very large classes of experiments.

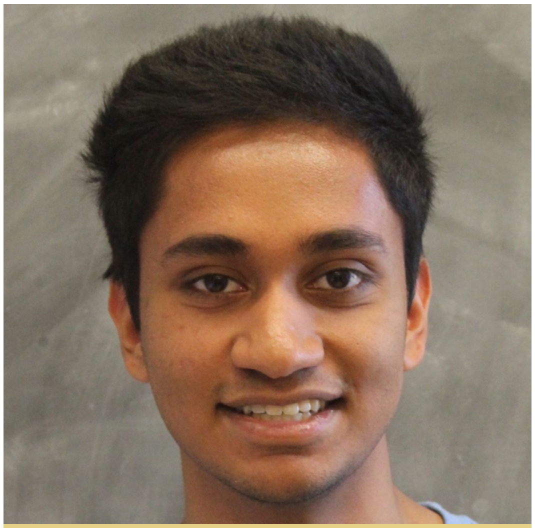

SUJIT RAO
CQE-LPS Doc Bedard Fellow. This three-year graduate fellowship is awarded through the MIT Center for Quantum Engineering. It is funded by the Laboratory of Physical Sciences and recognizes the achievements and technical leadership of Dr. Fernand (Doc) Bedard, a pioneer of cryogenic computing.

What are your future plans? We are currently in a fast-paced time where interesting research on quantum computing and information is being done in both academia and industrial labs. I plan to continue doing research, though with so many options it is hard to say exactly where I might go even in the short term.

Meet our MIT-CQE Principal Investigators

RAYMOND ASHOORI
Physics

MARC BALDO
EECS

JOHN BARRY
Lincoln Laboratory

KARL BERGGREN
EECS

RAFAEL GOMEZ-BOMBARELLI
DMSE

DON BORONSON
Lincoln Laboratory

DANIELLE BRAJE
Lincoln Laboratory

COLIN BRUZEWICZ
Lincoln Laboratory

PAOLA CAPPELLARO
NSE

MICHAEL CARBIN,
EECS

JOSEPH CHECKELSKY
Physics

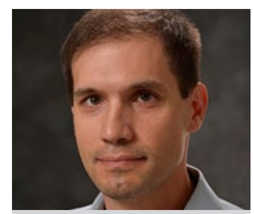

JOHN CHIAVERINI
Lincoln Laboratory

ISAAC CHUANG
EECS, Physics

RICCARDO COMIN
Physics

MICHAEL CUSUMANO
Sloan School

ERIC DAULER
Lincoln Laboratory

AROUND THE INSTITUTE

Meet our MIT-CQE Principal Investigators

DANE DEQUILETTES
Lincoln Laboratory

BENJAMIN DIXON
Lincoln Laboratory

DIRK ENGLUND
EECS

EDWARD FARHI
Physics

RICHARD FLETCHER
Physics

JOSEPH A. FORMAGGIO
Physics

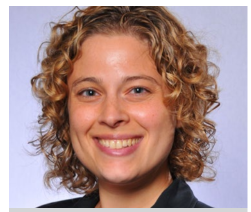

DANNA FREEDMAN
Chemistry

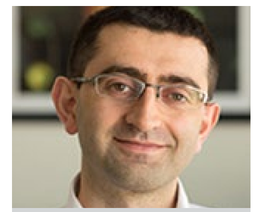

NUH GEDIK
Physics

MARK GOUKER
Lincoln Laboratory

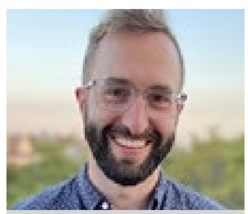

JEFF GROVER
RLE

SIMON GUSTAVSSON
RLE

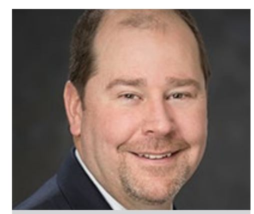

SCOTT HAMILTON
Lincoln Laboratory

SONG HAN
EECS

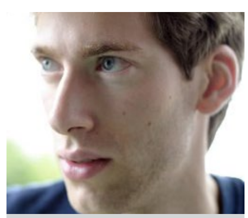

ARAM W. HARROW
Physics

PABLO JARILLO-HERRERO
Physics

LONG JU
Physics

Meet our MIT-CQE Principal Investigators

ANDREW J. KERMAN
Lincoln Laboratory

WOLFGANG KETTERLE
Physics

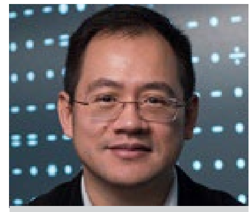

JU LI
NSE MSE

MINGDA LI
NSE

LUQIAO LIU
EECS

SETH LLOYD
ME, ES, Physics

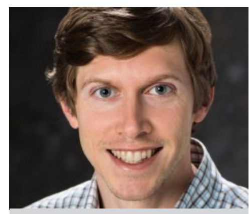

ROBERT McCONNELL
Lincoln Laboratory

ANAND NATARAJAN
EECS

FARNAZ NIROUI
EECS

JELENA NOTAROS
EECS

KEVIN OBENLAND
Lincoln Laboratory

KEVIN P. O'BRIEN
EECS

WILLIAM D. OLIVER
EECS, Physics, Lincoln Laboratory

TERRY ORLANDO
EECS

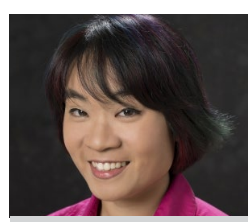

LINH PHAM
Lincoln Laboratory

RAJEEV RAM
EECS

MIT Center for Quantum Engineering

MIT Quantum Science and Engineering Consortium

Meet our MIT-CQE Principal Investigators

MOLLIE SCHWARTZ
Lincoln Laboratory

KYLE SERNIAK
Lincoln Laboratory

JEFFREY H. SHAPIRO
EECS

PETER SHOR
Mathematics

MICHAEL SIPSER
Mathematics

VIVISHEK SUDHIR
ME

TIMOTHY SWAGER
Chemistry

SENTHIL TODRARI
Physics

TROY VAN VOORHIS
Chemistry

VLADAN VULETIC
Physics

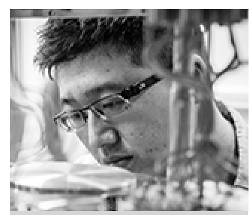

JOEL I-JAN WANG
RLE

LINDLEY WINSLOW
Physics

FRANCO N. C. WONG
RLE

WAYNE WOODS
Lincoln Laboratory

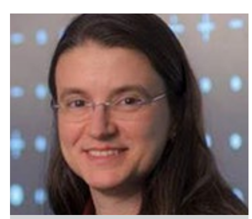

BILGE YILDIZ
NSE MSE

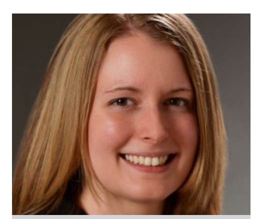

JONILYN YODER
Lincoln Laboratory

Meet our MIT-CQE Principal Investigators

MARTIN ZWIERLEIN
Physics

RAYMOND ASHOORI, *Physics*

“A long-sought regime of electronic behavior”
Raymond Ashoori
Nat. Mater. 21, 268–269 (2022)

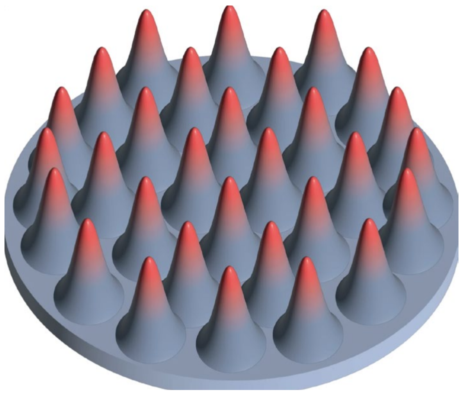

The particle density of an electron crystal.

A high-density electronic system contains a quantum fluid of electrons because electrons can lower their quantum energies by spreading their wave functions over long distances. Upon sufficiently lowering the electron density, a phase transition occurs in which Coulomb repulsion energies overcome quantum energies and electrons localize and space themselves out to form a crystal. The figure shows the particle density of such an electron crystal, with red colour demarcating high density. Other phases, such as emulsions of fluid and solid may exist near the transition, along with unusual magnetic and electronic behaviours.

KARL K. BERGGREN, *EECS*

“Reversible tuning of superconductivity in ion-gated niobium nitride ultrathin films by self-encapsulation with a high-κ dielectric layer”
Erik Piatti, Marco Colangelo, Mattia Bartoli, Owen Medeiros, Renato S. Gonnelli, Karl K. Berggren, Dario Daghero
arxiv.org/abs/2205.05491 (2022)

“Broadband Solenoidal Haloscope for Terahertz Axion Detection”
Jesse Liu, Kristin Dona, Gabe Hoshino, ... , Karl K. Berggren, et. al
PhysRevLett.128.131801 (2022) | arXiv:2111.12103 (2021)

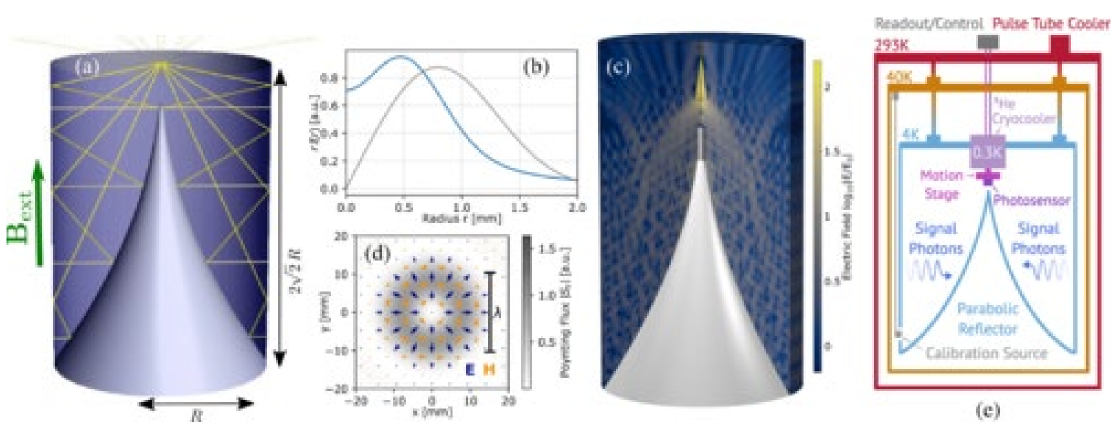

KARL K. BERGGREN, *EECS*

(a) BREAD reflector geometry: rays (yellow lines) emitted from the cylindrical barrel, which is parallel to an external magnetic field Bext from a surrounding solenoid (not shown) and focused at the vertex by a parabolic surface of revolution. (b) Radial intensity distribution rI(r) expected from DM velocity effects in the xy plane at the focal spot using ray tracing, for the BREAD geometry as in (a) with R=20 cm (blue) and for a conventional plane-parabolic mirror setup used in other experiments [69, 70, 71, 72, 73] with the same emitting surface area (gray). (c) Full field simulation at around 15 GHz including a preliminary coaxial horn design. (d) Electric (blue) and magnetic (orange) field distribution and time-averaged Poynting flux along the z direction in the xy plane at the focal spot. (e) Schematic setup in cryostat for pilot dark photon searches.

"Photon counting from the vacuum ultraviolet to the short wavelength infrared using semiconductor and superconducting technologies"
Jonathan Asaadi, Dan Baxter, Karl K. Berggren, et. al
arxiv.org/abs/2203.12542 (2022)

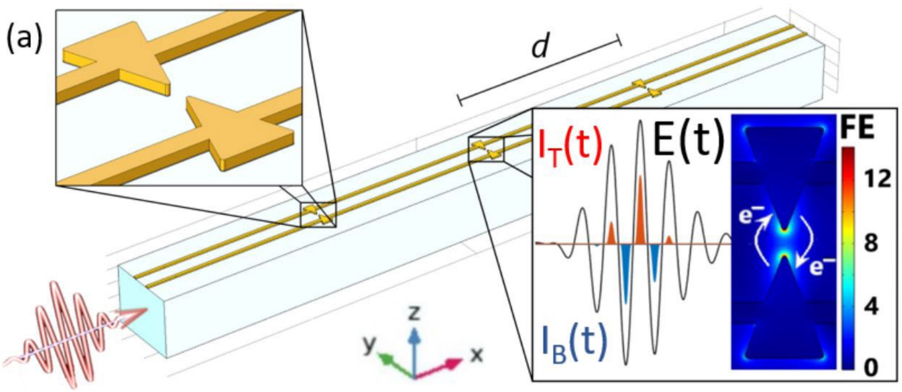

"PHz Electronic Device Design and Simulation for Waveguide-Integrated Carrier-Envelope Phase Detection"
Dario Cattozzo Mor, Yujia Yang, Felix Ritzkowsky, Franz X. Kärtner, Karl K. Berggren, Neetesh Kumar Singh, Phillip D. Keathley
ieeeXplore10.1109/JLT.2022.3150246 (2022) | arxiv.org/abs/2109.12558 (2021)

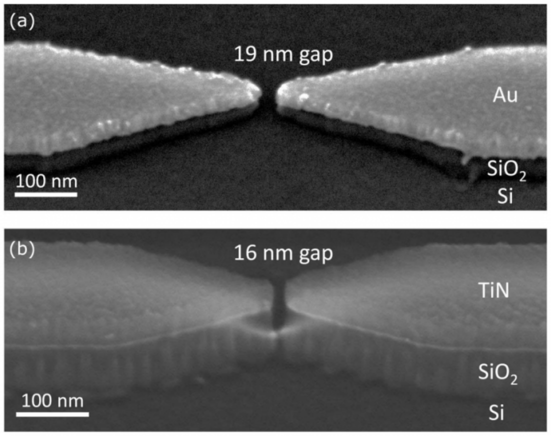

"Electron Emission Regimes of Planar Nano Vacuum Emitters"
Marco Turchetti, Yujia Yang, Mina R. Bionta, Alberto Nardi, Luca Daniel, Karl K. Berggren, Phillip D. Keathley
ieeeXplore 10.1109/TED.2022.3175706 (2022) | arxiv.org/abs/2201.04043 (2022)

From the Director
CQE PI Feature
CQE Student Feature
Around the Institute
Beyond the Institute
Quantum Conferences

KARL K. BERGGREN, *EECS*

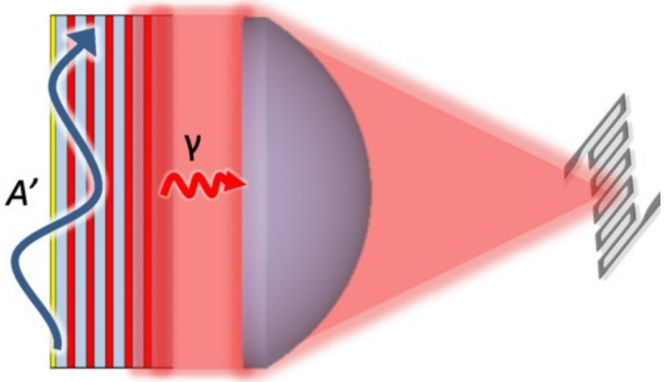

"New Constraints on Dark Matter from Superconducting Nanowires"
Yonit Hochberg, Benjamin V. Lehmann, Ilya Charaev, Jeff Chiles, Sae Woo Nam, Karl K. Berggren Phys. Rev. Lett. 128, 231802 (2022) | arxiv.org/abs/2110.01586 (2021)

Sketch of the LAMPOST concept. The dark photon dark matter field A′ converts to photons in a layered dielectric target. These photons are focused by a lens onto a small, low-noise SNSPD detector. The beam emitted from the stack is approximately uniform except for a small region in the middle where a mirror is absent, not shown here.

RAFAEL GOMEZ-BOMBARELLI, *DMSE*

"Excited state, non-adiabatic dynamics of large photoswitchable molecules using a chemically transferable machine learning potential"
Simon Axelrod, Eugene Shakhnovich, Rafael Gómez-Bombarelli
Nature Communications 13, Article number: 3440 (2022) | arxiv.org/abs/2108.04879 (2021)

Fig. 1: Depiction of the potential energy surfaces in azobenzene derivatives.

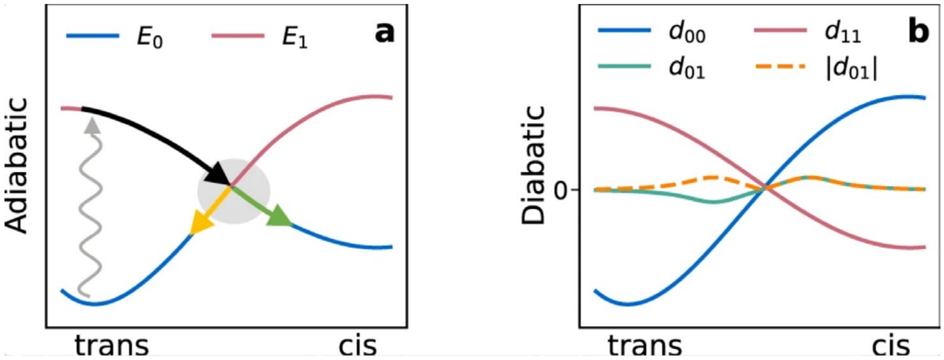

a S0 and S1 adiabatic energies, with the CI region shaded in gray. Initial excitation is shown with a vertical zigzag line. Trajectories prior to hopping are shown in black. Reactive and unreactive trajectories after hopping are shown in green and yellow, respectively. b Diabatic energies dnm≡(Hd)nmdnm≡(Hd)nm. The diagonal diabatic elements cross and become re-ordered along the isomerization coordinate. A CI occurs when the diagonal diabatic elements cross and the off-diagonal element becomes zero.

MIT Center for QuantumEngineering

MIT Quantum Science and Engineering Consortium

DANIELLE BRAJE, *Lincoln Laboratory*

“Thermally Polarized Solid-State Spin Sensor”

Reginald Wilcox, Erik Eisenach, John Barry, Matthew Steinecker, Michael O’Keeffe, Dirk Englund, and Danielle Braje

Phys. Rev. Applied 17, 044004 (2022) | arXiv:2109.01576 (2021)

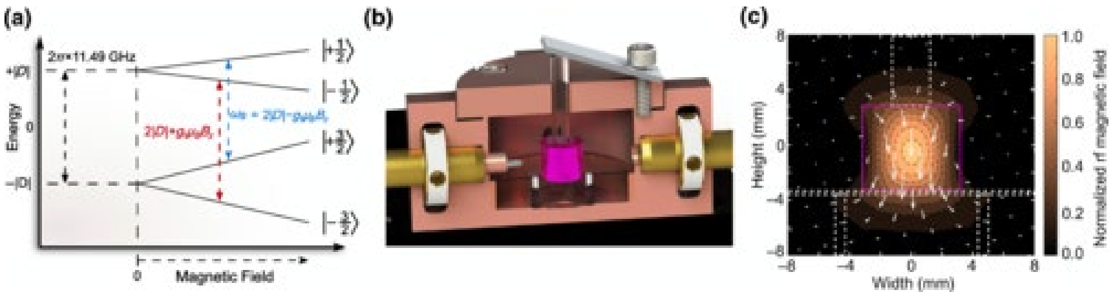

Ruby resonator design. (a) The electronic ground state of trivalent chromium (Cr^{3+}) in sapphire consists of two pairs of degenerate spin doublets separated by a 2π×11.49GHz zero-field splitting. External magnetic fields applied along the crystallographic c-axis lift the degeneracy of the |ms=±12⟩ and |ms=±32⟩ sublevels as shown, allowing the |ms=+32⟩↔|ms=+12⟩ transition with frequency ωs to be addressed spectroscopically. (b) Device cross section. Microwaves are coupled into the ruby resonator shown in pink, with a single probe loop on the left. While the shield supports up to four probe loops, only a single probe is used in this work. The ruby resonator is centered on a semi-insulating wafer of silicon carbide (SiC) and is clamped in place by a spring-loaded fused-silica tube. A copper shield encloses the ruby resonator and improves the resonator’s quality-factor by decreasing radiative losses. (c) Simulated rf magnetic field distribution of the ruby resonator’s TE01δ mode. The rf magnetic field is denoted by white arrows, the ruby resonator is outlined in pink, and the SiC and fused-silica support structures are indicated by white dashed lines.

PAOLA CAPPELLARO, *NSE*

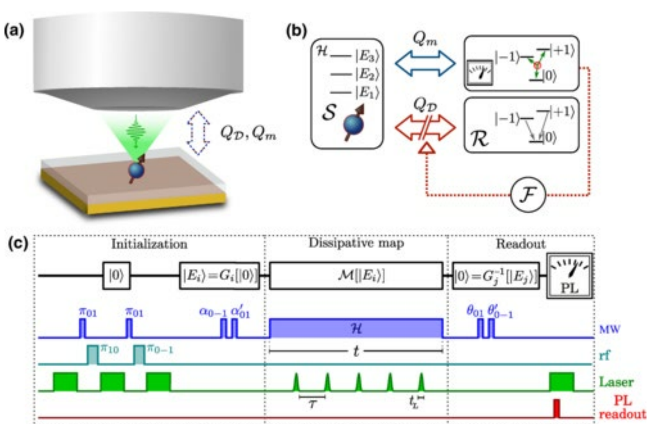

“Autonomous Dissipative Maxwell’s Demon in a Diamond Spin Qutrit”

S. Hernández-Gómez, S. Gherardini, N. Staudenmaier, F. Poggiali, M. Campisi, A. Trombettoni, F.S. Cataliotti, P. Cappellaro, and N. Fabbri

PRX Quantum 3, 020329 (2022) | arXiv:2105.14011 (2021)

(a),(b) Scheme of the spin system S in the presence of a green laser. On interaction with a laser pulse, the spin is subjected to a quantum measurement (Qm) of Sz, and dissipation (QD) toward the mS=0 spin projection. This irreversible dissipation is analogous to putting the system in contact with an out-of-equilibrium reservoir R. Since the interaction between the system and the reservoir is conditioned by the application

PAOLA CAPPELLARO, *NSE*

of a quantum measurement, the dissipation acts as an intrinsic feedback mechanism. The unitary part of the dynamics is defined by the Hamiltonian H, with eigenstates $|E_i\rangle$, *i=1,2,3. (c) Scheme to measure energy conditional probabilities. The stochastic dissipative map M is a combination of a train of NL equidistant short laser pulses and a continuous driving under the Hamiltonian H that can be either HNV or HMW (see the main text). The total time of the experiment* $t=N_L\tau$ *is defined in terms of the number of laser pulses and the time* τ *between them. The laser pulse duration tL is negligible with respect to the continuous driving. The gates* $G_i:|0\rangle\rightarrow|E_i\rangle$ *and* $G^{-1}_j:|E_j\rangle\rightarrow|0\rangle$ *enable one to prepare and read out the Hamiltonian eigenstates, respectively, by exploiting the optical properties of the NV center.*

"Characterizing temperature and strain variations with qubit ensembles for their robust coherence protection"

Guoqing Wang, Ariel Rebekah Barr, Hao Tang, Mo Chen, Changhao Li, Haowei Xu, Ju Li, Paola Cappellaro
arXiv:2205.02790 (2022)

"A geometric perspective: experimental evaluation of the quantum Cramer-Rao bound"

Changhao Li, Mo Chen, Paola Cappellaro
arXiv:2204.13777 (2022)

"Bias in Error-Corrected Quantum Sensing"

Ivan Rojkov, David Layden, Paola Cappellaro, Jonathan Home, and Florentin Reiter
Phys. Rev. Lett. 128, 140503 (2022) | arXiv:2101.05817 (2021)

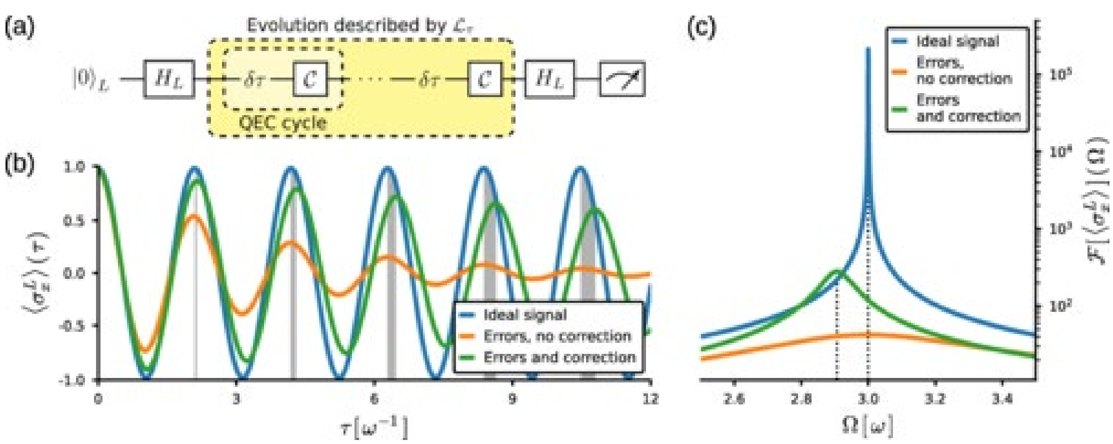

Bias in error-corrected quantum sensing. (a) Error-corrected Ramsey sequence represented as a quantum circuit where HL are logical Hadamard gates, C represents detection and correction processes and $\delta\tau$ *free evolution intervals under the signal with frequency* ω*. The overall dynamics during the sensing time* τ *is described by* L_τ*. In (b), we plot the expectation value* $\langle\sigma_{Lx}\rangle$ *as a function of the free evolution time* τ *for three different sensing models: ideal, uncorrected and error corrected. The parameters used for the simulation are* $\Gamma_{err}=0.1\omega$, $\Gamma_{qec}=5\omega$*. Panel (c) shows the Fourier transform F of the functions from Fig. 1.*

PAOLA CAPPELLARO, *NSE*

"A synthetic monopole source of Kalb-Ramond field in diamond"
Mo Chen, Changhao Li, Giandomenico Palumbo, Yan-Qing Zhu, Nathan Goldman, Paola Cappellaro
Science 375, 1017 (2022) | arXiv:2008.00596 (2020)

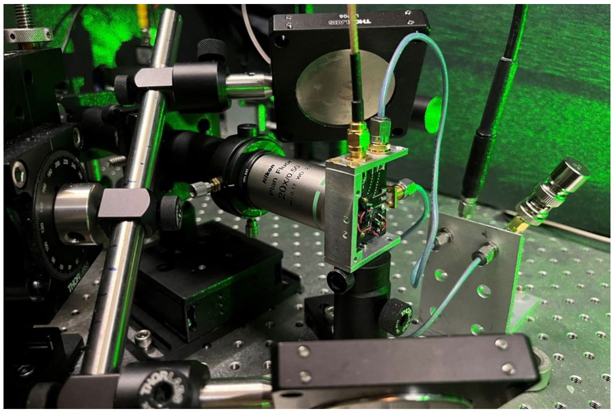

Sensing of Arbitrary-Frequency Fields Using a Quantum Mixer
Guoqing Wang, Yi-Xiang Liu, Jennifer M. Schloss, Scott T. Alsid, Danielle A. Braje, and Paola Cappellaro
MIT News (2022) | Phys. Rev. X 12, 021061 (2022)

MICHAEL CARBIN, *EECS*

"Tower: Data Structures in Quantum Superposition"
Charles Yuan, Michael Carbin
arXiv:2205.10255 (2022)

"SCOPE: Safe Exploration for Dynamic Computer Systems Optimization"
Hyunji Kim, Ahsan Pervaiz, Henry Hoffmann, Michael Carbin, Yi Ding
arXiv:2204.10451 (2022)

"Cello: Efficient Computer Systems Optimization with Predictive Early Termination and Censored Regression"
Yi Ding, Alex Renda, Ahsan Pervaiz, Michael Carbin, Henry Hoffmann
arXiv:2204.04831 (2022)

JOSEPH CHECKELSKY, *Physics*

"Band Structure Driven Thermoelectric Response of Topological Semiconductor ZrTe5"
Junbo Zhu, Changmin Lee, Fahad Mahmood, Takehito Suzuki, Shiang Fang, Nuh Gedik, Joseph G. Checkelsky
arXiv:2205.10394 (2022)

"Field-dependent Shubnikov-de Haas oscillations in ferromagnetic Weyl semi-metal Co3Sn2S2"
Linda Ye, Jorge I. Facio, Madhav P. Ghimire, Mun K. Chan, Jhih-Shih You, David C. Bell, Manuel Richter, Jeroen van den Brink, Joseph G. Checkelsky
arXiv:2203.04254 (2022)

JOHN CHIAVERINI, *Lincoln Laboratory*

"2022 Roadmap on integrated quantum photonics"
Galan Moody, Volker J Sorger, Daniel J Blumenthal, ..., John Chiaverini, et al
J. Phys. Photonics 4 012501 (2022) | arXiv:2102.03323 (2021)

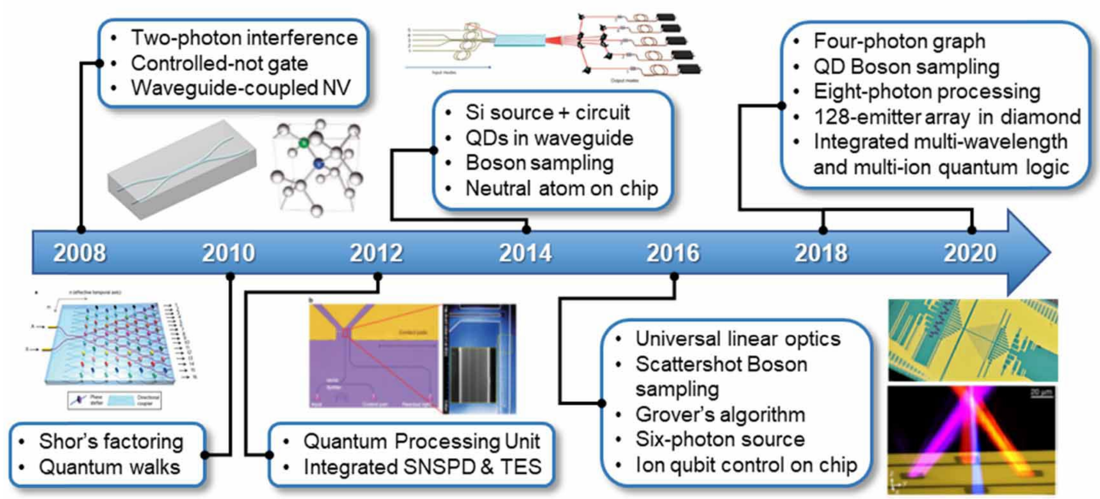

Key milestones in integrated quantum photonics in the past decade, beginning with two-photon interference and fundamental quantum gates prior to 2008 to large-scale devices comprising over 650 photonic components and arrays of deterministic and probabilistic quantum light sources on a single chip in 2020. Images reprinted with permission from the American Association for the Advancement of Science and Springer Nature.

ISAAC CHUANG, *EECS, Physics*

[“Quantum advantage for noisy channel discrimination”]

Zane M. Rossi, Jeffery Yu, Isaac L. Chuang, and Sho Sugiura

Phys. Rev. A 105, 032401 (2022) | arXiv:2105.08707 (2021)

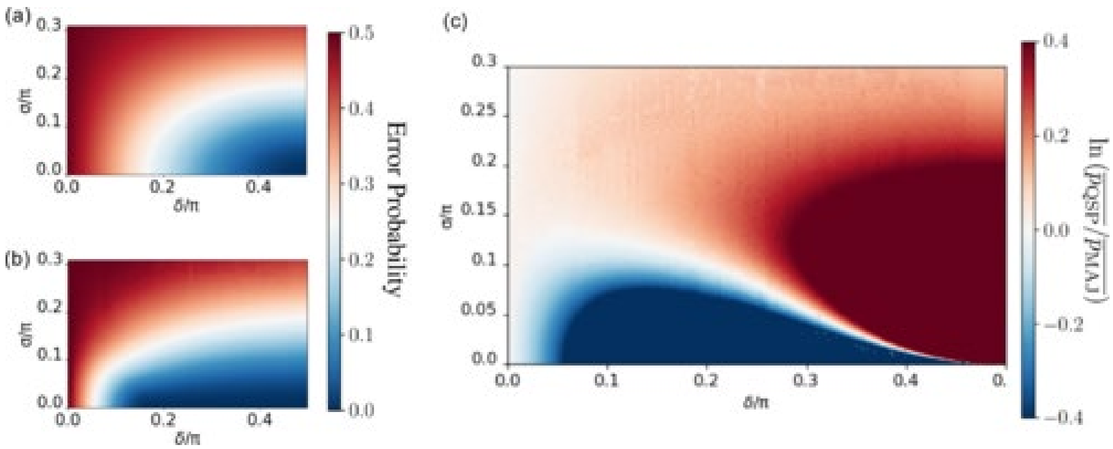

(a), (b) Error probabilities for MAJ-3 (a) and QSP-3 (b). In (c) is depicted the logarithm of the ratio of the error probability of MAJ-3 and that of QSP-3. Red is used for the area where MAJ-3 performs better, white indicates roughly equal performance, and blue indicates where QSP-3 performs better. Quantum advantage for coherent access protocols is present when both the “signal” (δ) and the “noise” (σ) are not too large.

“Pareto-optimal clustering with the primal deterministic information bottleneck”

Andrew K. Tan, Max Tegmark, Isaac L. Chuang

Entropy (2022)| arXiv:2204.02489 (2022)

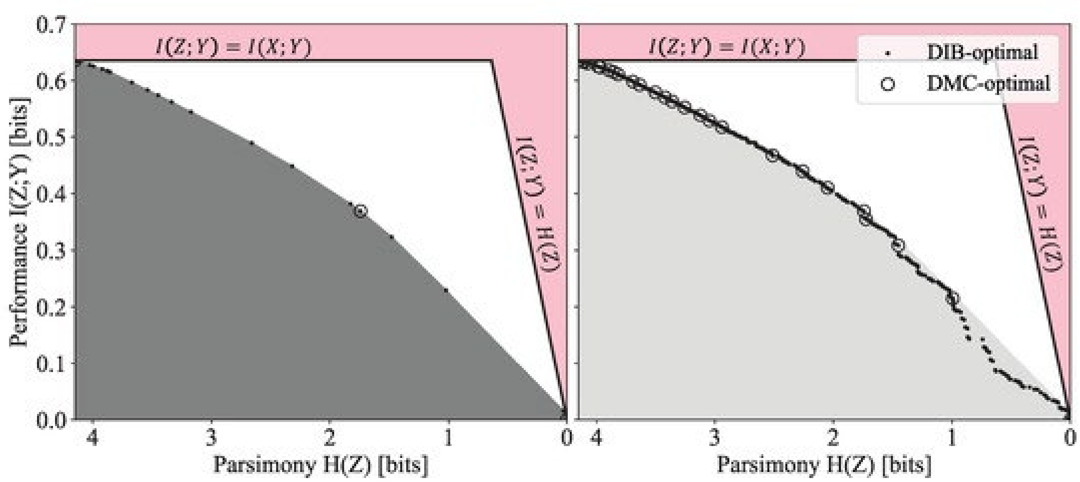

“Biological error correction codes generate fault-tolerant neural networks”

Alexander Zlokapa, Andrew K. Tan, John M. Martyn, Ila R. Fiete, Max Tegmark, Isaac L. Chuang

arXiv:2202.12887 (2022)

RICCARDO COMIN, *Physics*

[“Evidence for a single-layer van der Waals multiferroic”]

Q. Song*, C. A. Occhialini*, E. Ergeçen*, B. Ilyas*, D. Amoroso, P. Barone, J. Kapeghian, K. Watanabe, T. Taniguchi, A. S. Botana, S. Picozzi, N. Gedik, R. Comin

Nature 602, 601 (2022) | arXiv:2106.07661 (2021)

Crystal structure, magnetic order and optical characterization of bulk NiI2.

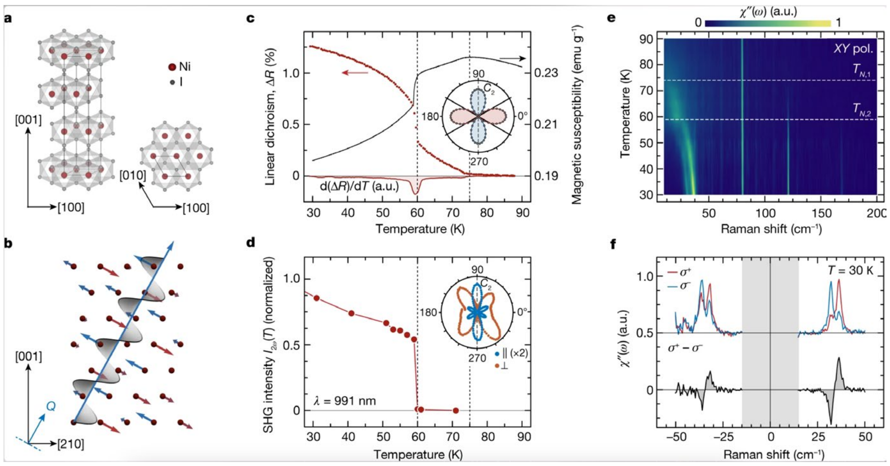

a, The high-temperature R3¯m-R3¯m structure of NiI2. b, The helical magnetic structure of bulk NiI2 below TN,2 = 59.5 K (see text). c, Temperature-dependent linear dichroism (ΔR(T)) measurements on a mono-domain region of bulk NiI2, overlaid on the magnetic susceptibility χmag. The inset shows the angular dependence of ΔR at T = 30 K; radial lines indicate the crystallographic a axes and the dashed line corresponds to the local C2 axis. d, Below band gap (λ = 991 nm) temperature-dependent SHG in bulk NiI2. The inset shows RA-SHG patterns for a monodomain region in the parallel (∥) and perpendicular (⊥)(⊥) polarization channels with the dashed line corresponding to the C2-axis orientation. Vertical dashed lines in c and d indicate the TN,1 and TN,2 transitions. e, Temperature-dependent Raman spectra in the XY polarization (pol.) channel. f, Circularly polarized Stokes and anti-Stokes Raman spectra of the soft mode excitations for σ+/σ− incident polarization (top) and the net ROA (σ+− σ−) (bottom). a.u., arbitrary units.

[“Carrier Doping Physics of Rare Earth Perovskite Nickelates RENiO3”]

J. Li, S. Ramanathan, R. Comin

Frontiers in Physics (2022)

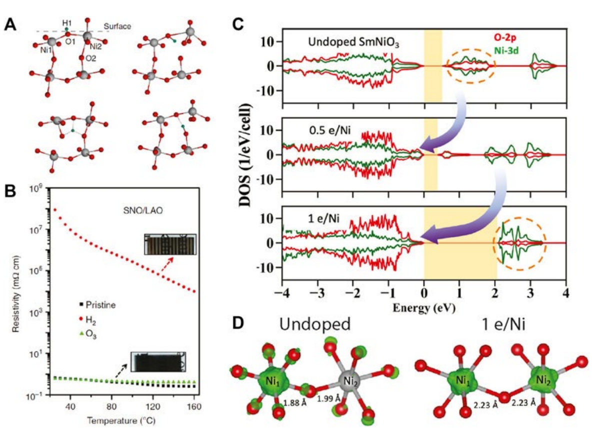

(A) The diffusive ionic intercalation process exemplified by hydrogen. The proton (H+, in green) mainly bonds with oxygen and undergoes diffusive rotation and transfer onto neighboring oxygen ions [35]. (B) Resistivity versus temperature for the pristine (black), hydrogen-intercalated (red), and ozone-annealed (green) SmNiO3 thin films grown on LaAlO3 substrates (SNO/LAO). The resistivity increases by eight orders of magnitude upon doping [19]. (C) Density of states of undoped and electron-doped SmNiO3. (D) The squared modulus of the unoccupied intermediated band wavefunctions (green isosurfaces) [dashed-circles in (D)] [38].

DANE DEQUILETTES, *Lincoln Laboratory*

"Slowed Recombination via Tunable Surface Energetics in Perovskite Solar Cells"
Dane W. deQuilettes, Jason Jungwan Yoo, Roberto Brenes, Felix Utama Kosasih, Madeleine Laitz, Benjia Dak Dou, Seong Sik Shin, Caterina Ducati, Moungi Bawendi, Vladimir Bulović
arXiv:2204.07642 (2022)

"Uncovering Temperature-Dependent Exciton-Polariton Relaxation Mechanisms in Perovskites"
Madeleine Laitz, Alexander E. K. Kaplan, Jude Deschamps, Ulugbek Barotov, Andrew H. Proppe, Inés García-Benito, Anna Osherov, Giulia Grancini, Dane W. deQuilettes, Keith Nelson, Moungi Bawendi, Vladimir Bulović
arXiv:2203.13816 (2022)

"Processing Induced Distinct Charge Carrier Dynamics of Bulky Organic Halide Treated Perovskites"
Benjia Dak Dou, Dane W. deQuilettes, Madeleine Laitz, Roberto Brenes, Lili Wang, Ella L Wassweiler, Richard Swartwout, Jason J. Yoo, Melany Sponseller, Noor Titan Putri Hartono, Shijing Sun, Tonio Buonassisi, Moungi G Bawendi, Vladimir Bulovic
arXiv:2203.05904 (2022)

DIRK ENGLUND, *EECS*

"Zero-Added-Loss Entangled Photon Multiplexing for Ground- and Space-Based Quantum Networks"
Kevin C. Chen, Prajit Dhara, Mikkel Heuck, Yuan Lee, Wenhan Dai, Saikat Guha, Dirk Englund
arXiv:2206.03670 (2022)

"Piezo-optomechanical cantilever modulators for VLSI visible photonics"
Mark Dong, David Heim, Alex Witte, Genevieve Clark, Andrew J. Leenheer, Daniel Dominguez, Matthew Zimmermann, Y. Henry Wen, Gerald Gilbert, Dirk Englund, Matt Eichenfield
APL Photonics 7, 051304 (2022)| arXiv:2201.12447 (2022)

DIRK ENGLUND, *EECS*

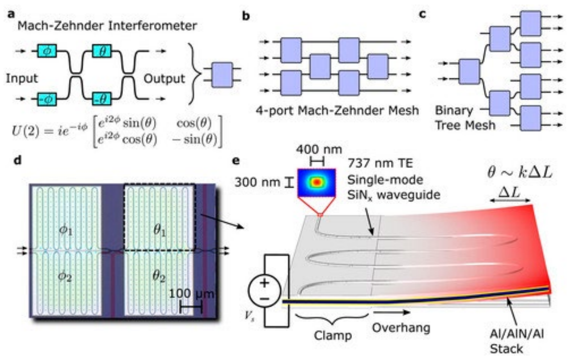

Piezo-optomechanical cantilevers for large-scale visible photonics: (a) diagram of a Mach–Zehnder interferometer with four phase shifters in push–pull configuration performing the U(2) operation; (b) schematic of a 4-port Mach–Zehnder mesh; (c) schematic of a 2 × 8 binary tree mesh; (d) optical microscope image of a fabricated device with four integrated cantilever phase shifters, each controlling the phases $\theta_{1,2}$, $\phi_{1,2}$; (e) operating principles of a piezo-optomechanical cantilever phase shifter, showing that an applied voltage V_s across an aluminum nitride piezo imparts a path-length change to the integrated SiN_x waveguides, inducing an effective phase shift θ.

"All-Photonic Artificial Neural Network Processor Via Non-linear Optics"
Jasvith Raj Basani, Mikkel Heuck, Dirk R. Englund, Stefan Krastanov
arXiv:2205.08608 (2022)

"Single-Shot Optical Neural Network"
Liane Bernstein, Alexander Sludds, Christopher Panuski, Sivan Trajtenberg-Mills, Ryan Hamerly, Dirk Englund
arXiv:2205.09103 (2022)

"A full degree-of-freedom photonic crystal spatial light modulator"
Christopher L. Panuski, Ian R. Christen, Momchil Minkov, Cole J. Brabec, Sivan Trajtenberg-Mills, Alexander D. Griffiths, Jonathan J.D. McKendry, Gerald L. Leake, Daniel J. Coleman, Cung Tran, Jeffrey St Louis, John Mucci, Cameron Horvath, Jocelyn N. Westwood-Bachman, Stefan F. Preble, Martin D. Dawson, Michael J. Strain, Michael L. Fanto, Dirk R. Englund
arXiv:2204.10302 (2022)

"Electric-Field Programmable Spin Arrays for Scalable Quantum Repeaters"
Hanfeng Wang, Matthew E. Trusheim, Laura Kim, Dirk R. Englund
arXiv:2204.07051 (2022)

"Routing Single Photons from a Trapped Ion Using a Photonic Integrated Circuit"
Uday Saha, James D. Siverns, John Hannegan, Mihika Prabhu, Qudsia Quraishi, Dirk Englund, Edo Waks
arXiv:2203.08048 (2022)

"Delocalized Photonic Deep Learning on the Internet's Edge"
Alexander Sludds, Saumil Bandyopadhyay, Zaijun Chen, Zhizhen Zhong, Liane Bernstein, Darius Bunandar, Matthew Streshinsky, Ari Novack, Tom Baehr-Jones, Michael Hochberg, Manya Ghobadi, Ryan Hamerly, Dirk Englund
arXiv:2203.05466 (2022)

DIRK ENGLUND, *EECS*

"Steady-state microwave mode cooling with a diamond NV ensemble"
Donald P. Fahey, Kurt Jacobs, Matthew J Turner, Hyeongrak Choi, Jonathan E. Hoffman, Dirk Englund, Matthew E. Trusheim
arXiv:2203.03462 (2022)

"Spin-Phonon-Photon Strong Coupling in a Piezomechanical Nanocavity"
Hamza Raniwala, Stefan Krastanov, Lisa Hackett, Matt Eichenfield, Dirk R. Englund, Matthew E. Trusheim
arXiv:2202.11291 (2022)

"A spin-optomechanical quantum interface enabled by an ultrasmall mechanical and optical mode volume cavity"
Hamza Raniwala, Stefan Krastanov, Matt Eichenfield, Dirk Englund
arXiv:2202.06999 (2022)

"Triggered single-photon generation and resonance fluorescence in ultra-low loss integrated photonic circuits"
Ashish Chanana, Hugo Larocque, Renan Moreira, Jacques Carolan, Biswarup Guha, Vikas Anant, Jin Dong Song, Dirk Englund, Daniel J. Blumenthal, Kartik Srinivasan, Marcelo Davanco
arXiv:2202.04615 (2022)

"Individually Addressable Artificial Atoms in Silicon Photonics"
Mihika Prabhu, Carlos Errando-Herranz, Lorenzo De Santis, Ian Christen, Changchen Chen, Dirk R. Englund
arXiv:2202.02342 (2022)

"Waveguide-Integrated Mid-Infrared Photodetection using Graphene on a Scalable Chalcogenide Glass Platform"
Jordan Goldstein, Hongtao Lin, Skylar Deckoff-Jones, Marek Hempel, Ang-Yu Lu, Kathleen A. Richardson,Tomas Palacios, Jing Kong, Juejun Hu, Dirk Englund
Nature Communications (2022) | arXiv.2112.14857 (2021)

"A Quantum Router Architecture for High-Fidelity Entanglement Flows in Multi-User Quantum Networks"
Yuan Lee, Eric Bersin, Axel Dahlberg, Stephanie Wehner, Dirk Englund
npj Quantum Information volume 8, Article number: 75 (2022) | arXiv:2005.01852 (2020)

DIRK ENGLUND, *EECS*

Components of a quantum repeater network.

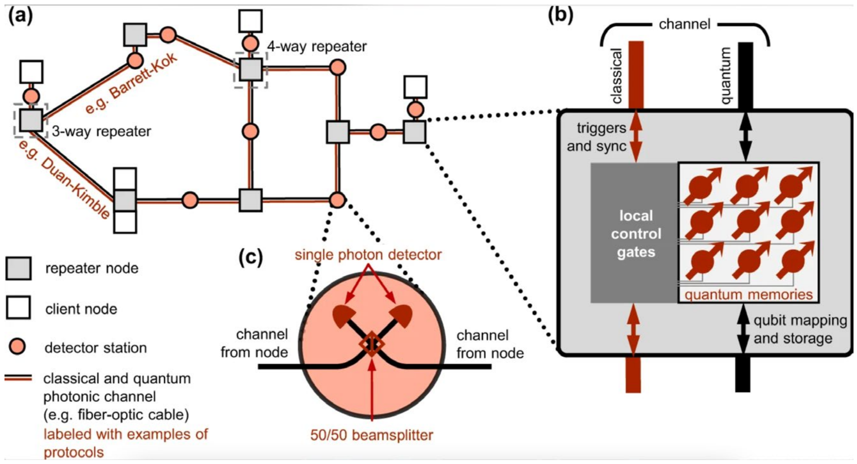

The quantum network comprises client nodes, which end users directly access, and repeater nodes, which connect clients by propagating entanglement through the network. a Physical layer implementation. In the physical layer4, repeater nodes may be connected by a variety of entanglement protocols. While all protocols require transmission of an entangled photon through a photonic channel, the specific protocol used in each link determines the physical configuration of these channels (e.g. optical fibers) and measurement devices associated with that link. Possible protocols include the cavity-mediated Duan–Kimble protocol9 and the photon emission-based Barrett–Kok5 and Cabrillo6 protocols. These latter protocols employ an intermediate detector station between nodes to herald successful entanglement. b Components in a repeater node. We classify repeater nodes based on the number of other nodes they connect to: a 4-way and a 3-way repeater are labeled. All adjacent repeater nodes are connected by quantum and classical channels (shown explicitly in black and light red respectively). c Detector station used in the photon emission-based protocols to herald entanglement.

JOSEPH A. FORMAGGIO, *Physics*

"Improved eV-scale Sterile-Neutrino Constraints from the Second KATRIN Measurement Campaign"

M. Aker, D. Batzler, A. Beglarian, ..., J. A. Formaggio, et al.
Phys. Rev. D 105, 072004 (2022) | arXiv:2201.11593 (2022)

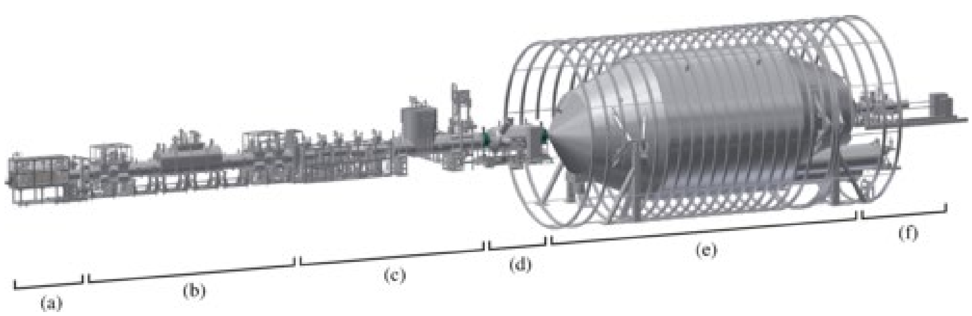

The KATRIN beamline is composed of six main components: (a) rear wall and electron gun, (b) windowless gaseous tritium source, (c) transport and pumping section, (d) prespectrometer, (e) main spectrometer, and (f) focal plane detector.

MIT Center for QuantumEngineering
MIT Quantum Science and Engineering Consortium

JOSEPH A. FORMAGGIO, *Physics*

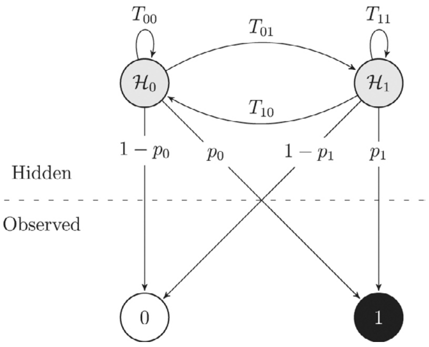

State diagram of HMM characteristic of CRES experiments. Hidden states (upper) produce observed data (lower) with different probabilities.

"Viterbi Decoding of CRES Signals in Project 8"
Ashtari Esfahani, Z. Bogorad, S. Böser, ..., J. A. Formaggio, et al.
New J. Phys. 24 053013 (2022) | arXiv:2112.05265 (2021)

"Toward CUPID-1T"
Armatol, ..., J. Formaggio, et. al
arXiv:2203.08386 (2022)

"KATRIN: Status and Prospects for the Neutrino Mass and Beyond"
M. Aker, ..., J. Formaggio, et. al
arXiv:2203.08059 (2022)

"Coherent elastic neutrino-nucleus scattering: Terrestrial and astrophysical applications"
M. Abdullah, ..., J. Formaggio, et. al
arXiv:2203.07361 (2022)

"The Project 8 Neutrino Mass Experiment"
Project 8 Collaboration, ..., J. Formaggio, et. al
arXiv:2203.07349 (2022)

"White Paper on Light Sterile Neutrino Searches and Related Phenomenology"
M. A. Acero, ..., J. Formaggio, et. al
arXiv:2203.07323 (2022)

"Optimization of the first CUPID detector module"
CUPID collaboration, ..., J. Formaggio, et. al
arXiv:2202.06279 (2022)

"EXCESS workshop: Descriptions of rising low-energy spectra"
P. Adari, ..., J. Formaggio, et. al
arXiv:2202.05097 (2022)

"New Constraint on the Local Relic Neutrino Background Overdensity with the First KATRIN Data Runs"
M. Aker, ..., J. Formaggio, et. al
arXiv:2202.04587 (2022)

DANNA FREEDMAN, *Chemistry*

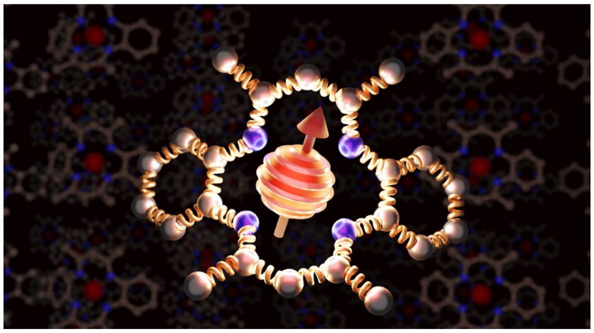

"Chemical Control of Spin-Lattice Relaxation to Create Room Temperature Molecular Qubit Candidates"
Amdur, M. J.; Mullin, K. R.; Waters, M. J.; Puggioni, D.; Wojnar, M. K.; Gu, M.; Sun, L.; Oyala, P. H.; Rondinelli, J. M.; Freedman, D. E.
Chem. Sci., 2022, DOI: 10.1039/D1SC06130E.

"Enhancing Spin Coherence in Optically Addressable Molecular Qubits through Host-Matrix Control"
SL Bayliss, P Deb, DW Laorenza, M Onizhuk, G Galli, DE Freedman, DD Awschalom
arXiv:2204.00168 (2022)

NUH GEDIK, *Physics*

"Dynamics of topological defects after a photo-induced melting of a charge-density wave"
Andrei E. Tarkhov, A. V. Rozhkov, Alfred Zong, Anshul Kogar, Nuh Gedik, Boris V. Fine
arXiv:2203.05001 (2022)

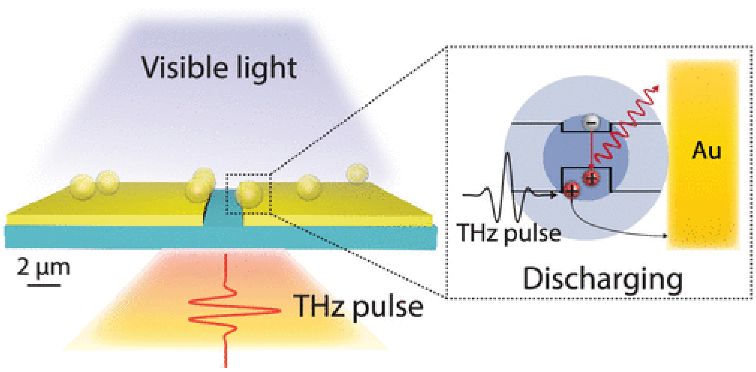

"Terahertz Field-Induced Reemergence of Quenched Photoluminescence in Quantum Dots"
Jiaojian Shi, Frank Y. Gao, Zhuquan Zhang, Hendrik Utzat, Ulugbek Barotov, Ardavan Farahvash, Jinchi Han, Jude Deschamps, Chan-Wook Baik, Kyung Sang Cho, Vladimir Bulović, Adam P. Willard, Edoardo Baldini, Nuh Gedik, Moungi G. Bawendi, Keith A. Nelson
Nano Lett. 2022, 22, 4, 1718–1725 | arXiv:2112.08533 (2021)

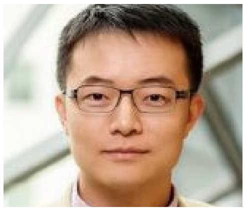

SONG HAN, *EECS*

"Variational Quantum Pulse Learning"
Zhiding Liang, Hanrui Wang, Jinglei Cheng, Yongshan Ding, Hang Ren, Zhengqi Gao, Xuehai Qian, Song Han, Weiwen Jiang, Yiyu Shi
arXiv:2203.17267 (2022)

"QOC: Quantum On-Chip Training with Parameter Shift and Gradient Pruning"
Hanrui Wang, Zirui Li, Jiaqi Gu, Yongshan Ding, David Z. Pan, Song Han
arXiv:2202.13239 (2022)

"PVNAS: 3D Neural Architecture Search with Point-Voxel Convolution"
Zhijian Liu, Haotian Tang, Shengyu Zhao, Kevin Shao, Song Han
arXiv:2204.11797 (2022)

ARAM W. HARROW, *Physics*

"Maximal entanglement velocity implies dual unitarity"
Tianci Zhou, Aram W. Harrow
arXiv:2204.10341 (2022)

"Efficient Classical Simulation of Random Shallow 2D Quantum Circuits"
John C. Napp, Rolando L. La Placa, Alexander M. Dalzell, Fernando G. S. L. Brandão, and Aram W. Harrow
Phys. Rev. X 12, 021021 (2022) | arXiv:2001.00021 (2020)

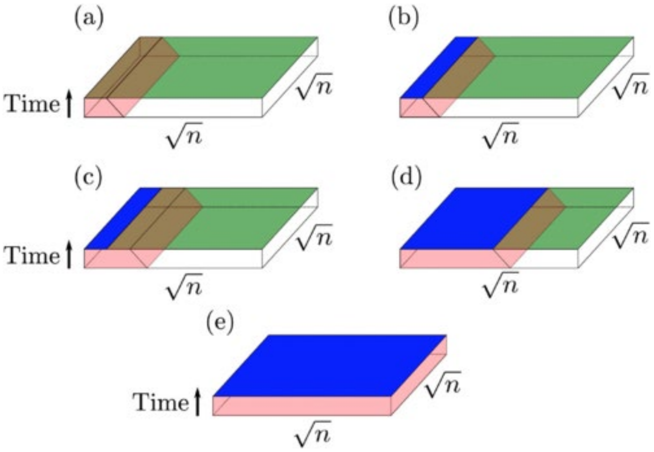

Schematic depiction of SEBD simulating a shallow 2D circuit. In all figures, the 2D circuit is depicted as a spacetime volume, with time flowing upward. The blue regions correspond to sites for which measurements have been simulated, while green regions correspond to unmeasured sites. In (a), we apply all gates in the light cone of column 1, namely, those gates intersecting the spacetime volume shaded red. In (b), we simulate the computational basis measurement of column 1. In (c), we apply all gates in the light cone of column 2 that were previously unperformed. (d) depicts the algorithm at an intermediate stage of the simulation, after the measurements of about half of the qudits have been simulated. The algorithm stores the current state as an MPS at all times, which may be periodically compressed to improve efficiency. (e) depicts the algorithm at completion: The measurements of all n of the qudits are simulated.

PABLO JARILLO-HERRERO, *Physics*

"Electrical switching of a moiré ferroelectric superconductor"
Dahlia R. Klein, Li-Qiao Xia, David MacNeill, Kenji Watanabe, Takashi Taniguchi, Pablo Jarillo-Herrero
arXiv:2205.04458 (2022)

"Terahertz-driven irreversible topological phase transition in two-dimensional MoTe2"
Jiaojian Shi, Ya-Qing Bie, Wei Chen, Shiang Fang, Jinchi Han, Zhaolong Cao, Takashi Taniguchi, Kenji Watanabe, Vladimir Bulović, Efthimios Kaxiras, Pablo Jarillo-Herrero, Keith A. Nelson
arXiv:1910.13609 (2022)

"Robust superconductivity in magic - angle multilayer graphene family"
Jeong Min Park, Yuan Cao, Li-Qiao Xia, Shuwen Sun, Kenji Watanabe, Takashi Taniguchi, Pablo Jarillo-Herrero
MIT News (2022) | Nature Materials (2022) | arXiv:2112.10760 (2021)

"Cyclotron resonance overtones and near-field magnetoabsorption via terahertz Bernstein modes in graphene"
D. A. Bandurin, E. Mönch, K. Kapralov, I. Y. Phinney, K. Lindner, S. Liu, J. H. Edgar, I. A. Dmitriev, P. Jarillo-Herrero, D. Svintsov, S. D. Ganichev
Nature Physics (2022) | arXiv:2106.02117

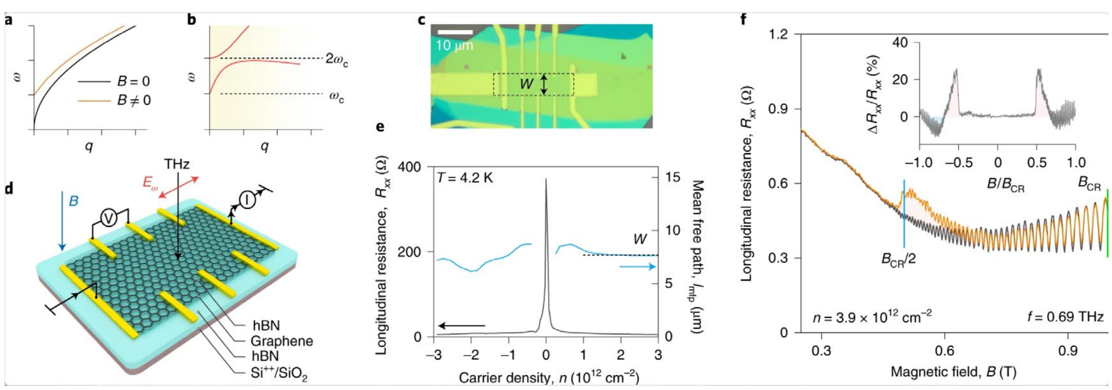

a, Dispersion of plasmons in a 2DES at zero and finite B. b, Dispersion of BMs. At large q ≳ 1/Rc, the magnetoplasmon dispersion splits into a series of branches with anticrossing regions in the vicinity of the cyclotron frequency harmonics. c, Optical photograph of an encapsulated graphene device. The yellow leads are gold contacts to graphene (dashed contour) and green colour corresponds to hBN. d, Measurement configuration: THz radiation is incident on doped graphene subjected to a perpendicular magnetic field. The photovoltage or photoresistance is measured between different pairs of contacts. e, Longitudinal resistance, Rxx, of the device shown in c as a function of carrier density at 4.2 K and B = 0, together with the corresponding mean free path, lmfp, obtained using the Drude model. f, Device resistance Rxx as a function of B measured in the dark (black curve) and in the presence of 0.69 THz radiation. The green and blue vertical lines correspond to the magnetic fields at which the CR and its second harmonics are expected at a given n. Inset, photoresistance ΔRxx normalized to Rxx as a function of B/BCR (T = 4.2 K).

LONG JU, *Physics*

[“Spectroscopy Signatures of Electron Correlations in a Trilayer Graphene/hBN Moiré Superlattice”]

J. Yang, G. Chen, T. Han, Q. Zhang, Y-H. Zhang, L. Jiang, B. Lyu, H. Li, K. Watanabe, T. Taniguchi, Z. Shi, T. Senthil, Y. Zhang, F. Wang, L. Ju

Science (2022) | arXiv:2202.12330 (2022)

Device structure and interband optical transitions in an ABC-stacked TLG/hBN moiré superlattice.

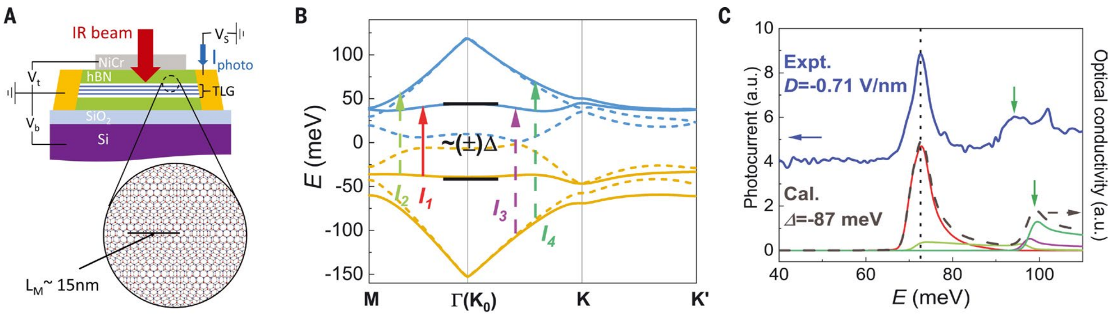

(A) Illustration of a dual-gated TLG device with a moiré wavelength of ~15 nm. IR, infrared; Vb, bottom-gate voltage; Vt, top-gate voltage; Vs, source-drain voltage. (B) Calculated band structure of TLG in the mini-Brillouin zone under a moiré potential (30). Dashed curves represent minibands at zero displacement field, whereas solid curves indicate minibands at a displacement field induced by gates so that Δ = −87 meV. Δ represents the gate-induced potential difference between the top and bottom layer of TLG. Arrows labeled as I1 to I4 represent interband optical transitions when the Fermi level is inside the gap. (C) The photocurrent spectrum of TLG/hBN at a displacement field D = −0.71 V/nm and calculated optical conductivity spectrum at Δ = −87 meV. Calculated contributions from transitions I1 to I4 are plotted as solid curves, and the sum is plotted as a dashed curve. The prominent experimental peak at ~72 meV (indicated by the vertical dashed line) corresponds to transition I1. The peak in the photocurrent spectrum indicated by a green arrow corresponds to the peak in optical conductivity that is dominated by I3 and I4. All photocurrent spectroscopy measurements were performed at a sample temperature of 2 K. a.u., arbitrary units; Cal., calculated; Expt., experimental.

ANDREW J. KERMAN, *Lincoln Laboratory*

[“Superconducting-semiconducting voltage-tunable qubits in the third dimension”]

Thomas M. Hazard, Andrew J. Kerman, Kyle Serniak, Charles Tahan

arXiv:2203.06209 (2022)

WOLFGANG KETTERLE, *Physics*

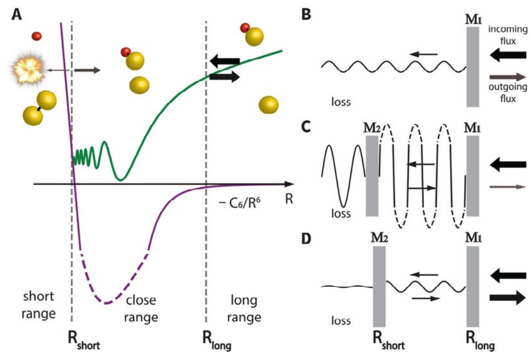

[“Control of reactive collisions by quantum interference”]

Hyungmok Son, Juliana J. Park, Yu-Kun Lu, Alan O. Jamison, Tijs Karman, Wolfgang Ketterle
MIT Press Release (2022) | U Waterloo Press Release (2022)| Science 375 , 1006–1010 (2022) | Chemistry World | arXiv:2109.03944 (2021)

Quantum interference in atom-molecule collisions can be understood by an optical analogy. On the right side, a laser beam is partially transmitted and reflected by two-mirrors. How much light reaches the left side depends on how the multiple reflections interfere. Similarly, in the atom-molecule collision studied at MIT (left), a Na atom (yellow sphere) and a NaLi molecule (yellow and red spheres) can be reflected or transmitted at long and at close distances, and the multiple bounces interfere.

“Preparation of the spin-Mott state: A spinful Mott insulator of repulsively bound pairs”

Julius de Hond, Jinggang Xiang, Woo Chang Chung, Enid Cruz-Colón, Wenlan Chen, William Cody Burton, Colin J. Kennedy, Wolfgang Ketterle
Phys. Rev. Lett. 128 , 093401 (2022) | arXiv:2110.00354 (2021)

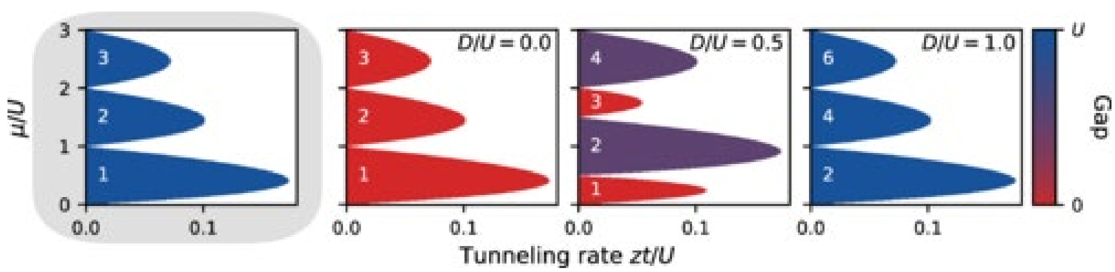

Mean-field phase diagram of the (two-component) Mott insulator showing the number of atoms per site for a chemical potential μ and tunneling rate t (which, in the mean-field model, is enhanced by the coordination number z). The leftmost panel contains the phase diagram of the single-component system [23]. The other panels, from left to right, show the two-component phase diagram for D/U=0, 0.5, and 1.0. As D increases, the lobes with an uneven number of particles shrink until they vanish because the absence of interactions leads to the formation of two independent Mott insulators. The lobe color indicates the excitation gap. In the single-component system, the first-excited state is a particle-hole pair, which costs an energy U to create. In the two-component system it is a spin excitation with an energy on the order of D. The numbers in the lobes indicate ⟨n⟩=⟨na⟩+⟨nb⟩.

“Fast optical transport of ultracold molecules over long distances”

Yicheng Bao, Scarlett S. Yu, Loïc Anderegg, Sean Burchesky, Derick Gonzalez-Acevedo, Eunmi Chae, Wolfgang Ketterle, Kang-Kuen Ni, John M. Doyle
arXiv:2205.06334 (2022)

“Observation of bosonic stimulation in light scattering”

Yu-Kun Lu, Yair Margalit, Wolfgang Ketterle
arXiv:2204.06639 (2022)

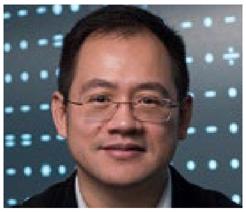

JU LI, *NSE MSE*

“First-principles Calculation of the Temperature-dependent Transition Energies in Spin Defects”
Hao Tang, Ariel Rebekah Barr, Guoqing Wang, Paola Cappellaro, Ju Li
arXiv:2205.02791 (2022)

“Abnormal Surface Nonlinear Optical Responses in Topological Materials”
Haowei Xu, Hua Wang, Ju Li
npj Computational Materials (2022) | arXiv:2109.05592 (2021)

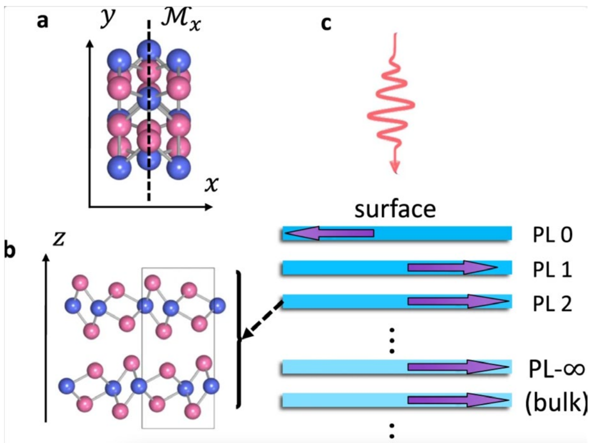

Illustration of Td-WTe2 under light illumination.

a, b Atomic structure of Td-WTe2. The dashed line in a denotes the mirror-x symmetry MxMx of Td-WTe2. c A sketch of materials under light illumination. The surface and bulk principal layer (PL) corresponds to PL-0 and PL-∞, respectively. The optical responses of the surface and the bulk can be distinct (indicated by the purple arrows). For Td-WTe2, each PL consists of two WTe2 layer without inversion symmetry as shown in b.

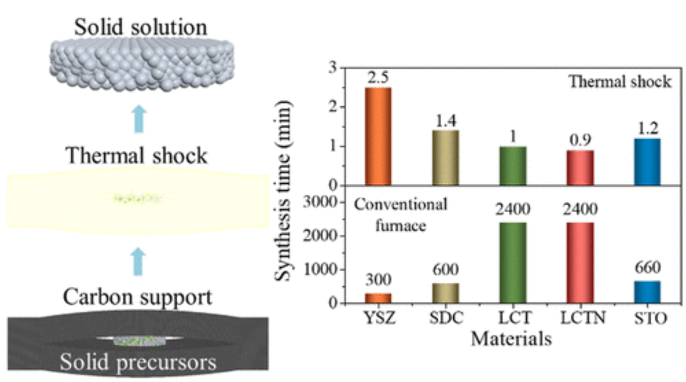

“Synthesizing Functional Ceramic Powders for Solid Oxide Cells in Minutes through Thermal Shock”
Weiwei Fan, Zhichu Ren, Zhu Sun, Xiahui Yao, Bilge Yildiz, Ju Li
ACS Energy Letters, 7, 13, 1223-1229, (2022)

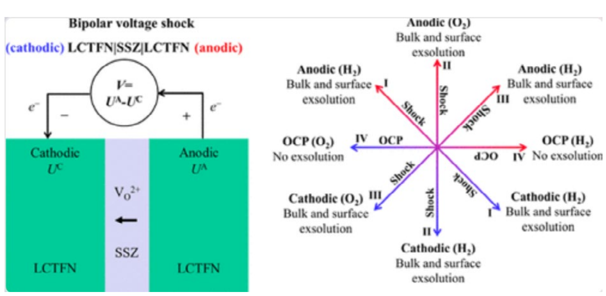

“Anodic Shock-Triggered Exsolution of Metal Nanoparticles from Perovskite Oxide”
Weiwei Fan, Baoming Wang, Rui Gao, Georgios Dimitrakopoulos, Jiayue Wang, Xianghui Xiao, Lu Ma, Kai Wu, Bilge Yildiz and Ju Li
Journal of the American Chemical Society, 144, 17, 7657–7666 (2022)

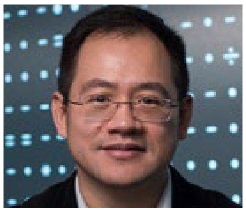

JU LI, *NSE MSE*

"Battery degradation prediction against uncertain future conditions with recurrent neural network enabled deep learning"
Jiahuan Lu, Rui Xionga, Jinpeng Tiana, Chenxu Wanga, Chia-Wei Hsu, Nien-Ti Tsou, Fengchun Sun, Ju Li
Energy Storage Materials (2022)

"TeaNet: Universal neural network interatomic potential inspired by iterative electronic relaxations"
So Takamoto, Satashi Izumi, Ju Li
Computational Materials Science 207, 111280 (2022)

"Machine learning in nuclear materials research"
D Morgan, G Pilania, A Couet, BP Uberuaga, C Sun, J Li
Current Opinion in Solid State and Materials Science 26 (2), 100975 (2022)

"Learning constitutive relations of plasticity using neural networks and full-field data"
Y Zhang, QJ Li, T Zhu, J Li
Extreme Mechanics Letters 52, 101645 (2022)

"Acid-in-clay electrolyte for wide-temperature-range and long-cycle proton batteries"
Shitong Wang,Heng Jiang,Yanhao Dong, ..., Ju Li
Advanced Materials, (2022)

Machine learning of metal-ceramic wettability
So Yeon Kim, Ju Li
Journal of Materiomics 8 (1), 195-203 (2022)

"Generalized Wilson Loop Method for Nonlinear Light-Matter Interaction"
Hua Wang, Xiuyu Tang, Haowei Xu, Ju Li, Xiaofeng Qian
Npj quantum materials (2022) | arXiv:2206.04560 (2022)

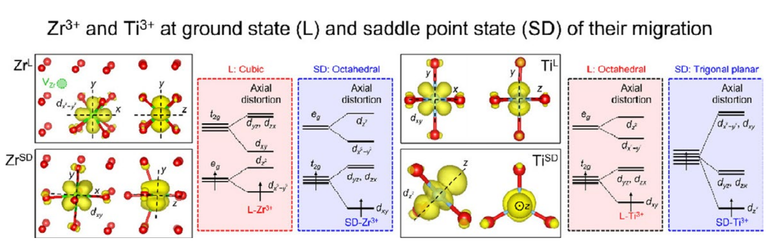

"Enhanced mobility of cations and anions in the redox state: The polaronium mechanism"
Y Dong, L Qi, A Alvarez, J Li, IW Chen
Acta Materialia 232, 117941 (2022)

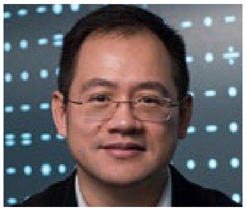

JU LI, *NSE MSE*

“In situ TEM visualization of LiF nanosheet formation on the cathode-electrolyte interphase (CEI) in liquid-electrolyte lithium-ion batteries”
Q Zhang, J Ma, L Mei, J Liu, Z Li, J Li, Z Zeng
Matter 5 (4), 1235-1250 (2022)

“Revitalizing interface in protonic ceramic cells by acid etch”
Wenjuan Bian, Wei Wu, Baoming Wang, Wei Tang, Meng Zhou, Congrui Jin, Hanping Ding, Weiwei Fan, Yanhao Dong, Ju Li & Dong Ding
Nature 604 (7906), 479-485 (2022)

“Charging sustainable batteries”
Christian Bauer, ..., Ju Li, ... et. al
Nature Sustainability 5 (3), 176-178 (2022)

“Rejuvenation of plasticity via deformation graining in magnesium”
Bo-Yu Liu, Zhen Zhang, Fei Liu, ..., Ju Li, et. al
Nature communications 13 (1), 1-10 (2022)

“Thermally drawn rechargeable battery fiber enables pervasive power”
T Khudiyev, B Grena, G Loke, ..., Ju Li, et. al
Materials Today 52, 80-89 (2022)

“Cryo-Electron Tomography of Highly Deformable and Adherent Solid-Electrlyte Interphase Exoskeleton in Li-Metal Batteries with Ether-based Electrolyte”
Bing Han, Xiangyan Li, Qi Wang, Yucheng Zou, ..., Ju Li, et. al
Advanced Materials, 2108252 (2022)

MINGDA LI, *NSE*

“Panoramic mapping of phonon transport from ultrafast electron diffraction and machine learning”
Z. Chen, X. Shen, N. Andrejevic, T. Liu, D. Luo, T. Nguyen, N. C. Drucker, M. Kozina, Q. Song, C. Hua, G. Chen, X. Wang, J. Kong, and M Li
arXiv:2202.06199 (2022)

“Machine learning spectral indicators of topology”
N. Andjejevic, J. Andrejevic, C. H. Rycroft and M. Li
arXiv:2003.00994 (2022)

MINGDA LI, *NSE*

[“Elucidating proximity magnetism through polarized neutron reflectometry and machine learning”]

N. Andrejevic, Z. Chen, T. Nguyen, L. Fan, H. Heiberger, V. Lauter, L-J Zhou, Y-F Zhao, C-Z Chang, A. Grutter, and M Li

App. Phys. Rev. 9, 011421 (2022) | arXiv:2109.08005 (2021)

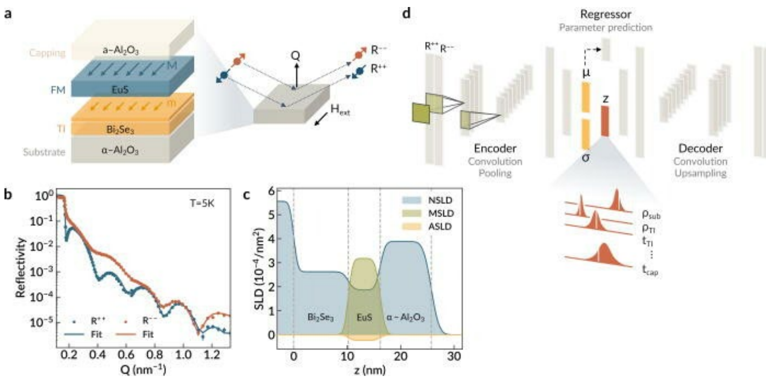

VAE with regression for PNR data analysis. (a) Schematic illustration of the proximity-coupled Bi2Se3/EuS system. A depiction of the spin-polarized neutron reflectometry experiment under an externally applied magnetic field is shown at right. (b) Reflectometry profile of the heterostructure in (a) measured at T = 5 K. Solid lines correspond to a representative fit obtained using the GenX parameter refinement program. Error-bars represent 1 standard deviation. (c) Nuclear, magnetic, and absorption SLD profiles corresponding to the fit in (b). (d) Schematic illustration of the VAE architecture used for PNR parameter retrieval.

[“Electronic properties of correlated kagomé metals AV3Sb5 (A = K, Rb, Cs): A perspective”]

Thanh Nguyen and Mingda Li

J. Appl. Phys. 131, 060901 (2022) | arXiv:2109.06809 (2021)

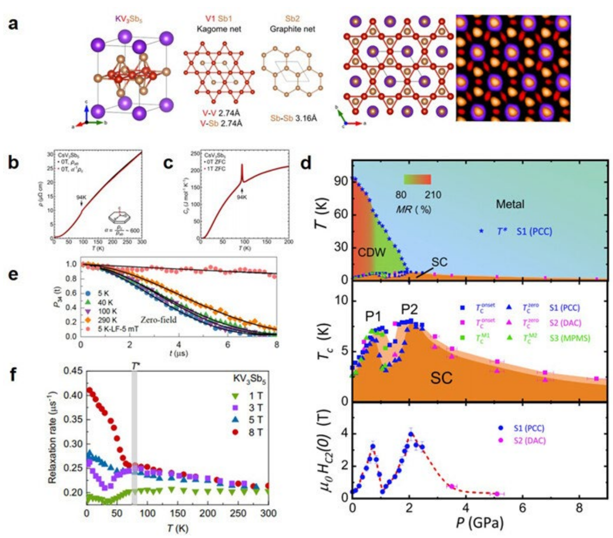

Crystal structure, double-dome superconductivity, and µμSR measurements. (a) Crystal structure of AV3Sb5AV3Sb5 formed by a vanadium (V) kagomé net, two distinct antimony (Sb) sublattices, intercalated by a layer of alkali atoms. (b) Electrical resistivity and (c) heat capacity measurements of CsV3Sb5CsV3Sb5 demonstrating an anomaly near 94 K associated with charge ordering. (d) Pressure–temperature phase diagram of CsV3Sb5CsV3Sb5 displaying charge density wave ordering (CDW) and superconductivity (SC) (top). Plots of the superconducting transition temperature TcTc (middle) and of the upper critical field at zero temperature µ0HC2(0)µ0HC2(0) (bottom) as a function of pressure both display features of double-dome superconductivity. PCC, piston cylinder cell; DAC, diamond anvil cell; MPMS, MPMS-5T, Quantum Design. (e) Zero field µμSR time spectra of KV3Sb5KV3Sb5 at different temperatures with black lines serving as fits to a depolarization function. (f) Plot of the muon spin relaxation rate as a function of temperature under the cc-axis at different magnetic fields. The gray line represents the charge ordering temperature T∗T∗. (a)–(c) from Ref. 2, (d) from Ref. 26, and (e)–(f) from Ref. 27.

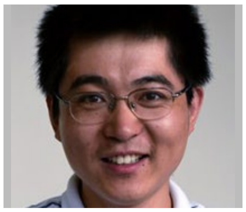

LUQIAO LIU, *EECS*

“Tunable Magnonic Chern Bands and Chiral Spin Currents in Magnetic Multilayers”
Zhongqiang Hu, Liang Fu, Luqiao Liu
Phys. Rev. Lett. 128, 217201 (2022) | arXiv:2201.00312 (2022)

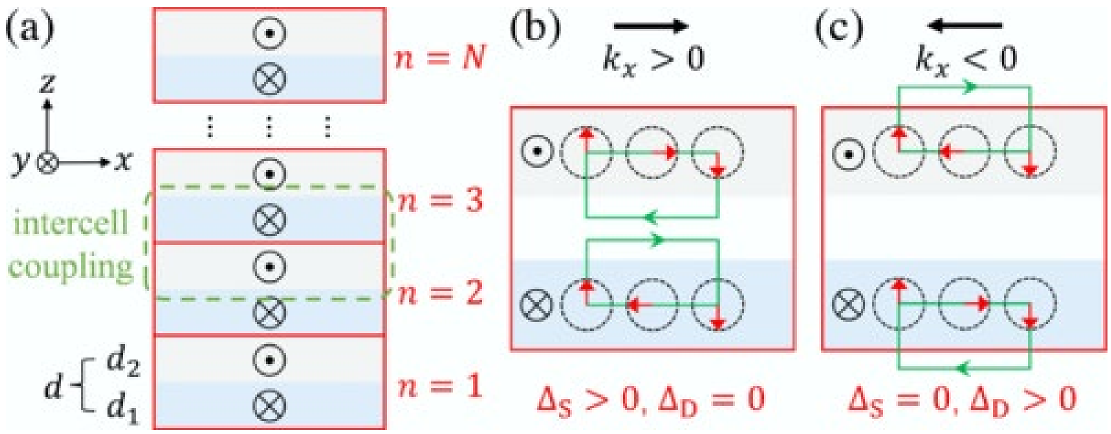

(a) Scheme of antiparallelly aligned magnetic multilayers. The blue (gray) blocks with thickness of d1(2) form the 1st (2nd) sublattice. The equilibrium moments in the 1st (2nd) sublattice are parallel to the +y (−y) direction, represented by ⊗ (⊙) symbols. The red, solid frames correspond to unit cells (indexed by n=1,2,...,N) with thickness of d=d1+d2. The green, dotted frames select two layers belonging to neighboring cells with intercell dipolar coupling. (b) Scheme of dipolar fields (green lines and arrows) generated by propagating magnons with kx>0 in two layers within a cell. The red arrows represent the deviations of magnetic moments from their equilibrium orientations, which propagates from left to right as a function of time (the traces are represented by black, dotted circles). Here, the two layers experience finite dipolar fields from each other, corresponding to ΔS>0. Meanwhile, they experience zero dipolar fields from magnons in the layers of neighboring cells, corresponding to ΔD=0. (c) Scheme of dipolar fields generated by propagating magnons with kx<0 for two layers within a cell, corresponding to ΔS=0 and ΔD>0.

SETH LLOYD, *ME, ES, Physics*

“Geometric Event-Based Relativistic Quantum Mechanics”
Vittorio Giovannetti, Seth Lloyd, Lorenzo Maccone
arXiv:2206.08359 (2022)

“Measuring magic on a quantum processor”
Salvatore F. E. Oliviero, Lorenzo Leone, Alioscia Hamma, Seth Lloyd
arXiv:2204.00015 (2022)

“projUNN: efficient method for training deep networks with unitary matrices”
Bobak Kiani, Randall Balestriero, Yann Lecun, Seth Lloyd
arXiv:2203.05483 (2022)

SETH LLOYD, *ME, ES, Physics*

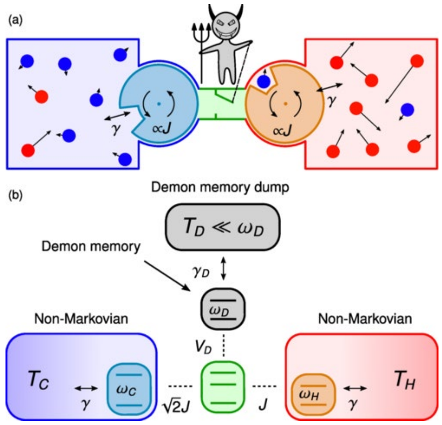

“Quantum Maxwell’s demon assisted by non-Markovian effects”

Kasper Poulsen, Marco Majland, Seth Lloyd, Morten Kjaergaard, and Nikolaj T. Zinner
Phys. Rev. E 105, 044141 (2022) | arXiv:2108.08855 (2021)

(a) Classical analog of the demon setup where rotating wheels illustrate the added predictability of a non-Markovian bath. (b) Illustration of the demon setup where two non-Markovian baths are connected by a qutrit. The cold non-Markovian bath consists of a qubit whose correlation functions decay due to the Markovian bath of temperature TC and likewise for the non-Markovian hot bath. A third qubit is demon memory, which can decay through interaction with the memory dump.

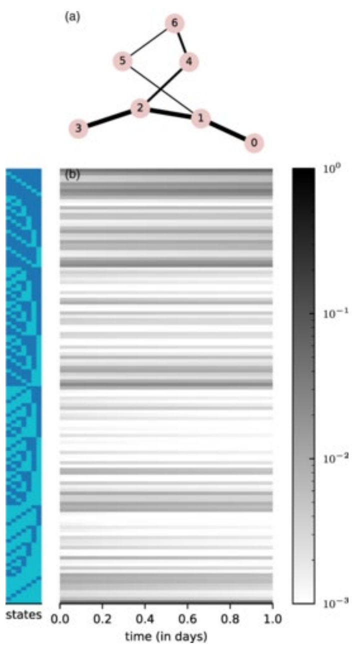

“Quantum advantage for differential equation analysis”

Bobak Toussi Kiani, Giacomo De Palma, Dirk Englund, William Kaminsky, Milad Marvian, and Seth Lloyd
Phys. Rev. A 105, 022415 (2022) | arXiv:2010.15776 (2020)

(a) Seven-node network used for simulation of the continuous-time Markov chain. Line widths correspond to the rate of infection from infected neighbor nodes (rSI={0.4,0.8,1.6} from thinnest to thickest lines). The network has the feature that some nodes (e.g., nodes 2 and 3) are strongly connected to neighboring nodes and others (e.g., node 5) are not. (b) Probabilities of Markov states over the course of three days shown as a color-bar chart (logarithmically scaled). Postprocessing is performed on the data between days 1 and 2 contained in the orange box. States are enumerated as rows on the left-hand side, each denominated by a seven-node color bar numbered node 0 on the left to node 6 on the right. Dark and light colors indicate that a node in that state is infected and susceptible, respectively.

“Learning quantum data with the quantum Earth Mover’s distance”

Bobak Toussi Kiani, Giacomo De Palma, Milad Marvian, Zi-Wen Liu and Seth Lloyd
IOPScience Quantum Science and Technology (2022) | arXiv:2101.03037 (2021)

“Quantum Algorithm for Petz Recovery Channels and Pretty Good Measurements”

András Gilyén, Seth Lloyd, Iman Marvian, Yihui Quek, and Mark M. Wilde
Phys. Rev. Lett. 128, 220502 (2022) | arXiv:2006.16924 (2020)

FARNAZ NIROUI, *EECS*

"A High-Lift Micro-Aerial-Robot Powered by Low-Voltage and Long-Endurance Dielectric Elastomer Actuators"
Zhijian Ren, Suhan Kim, Xiang Ji, Weikun Zhu, Farnaz Niroui, Jing Kong, Yufeng Chen
Adv. Mater. (2022)

JELENA NOTAROS, *EECS*

"Integrated Visible-Light Liquid-Crystal-Based Phase Modulators"
M. Notaros, T. Dyer, M. Raval, C. Baiocco, J. Notaros, and M. R. Watts
Optics Express 30(8), 13790-13801 (2022)

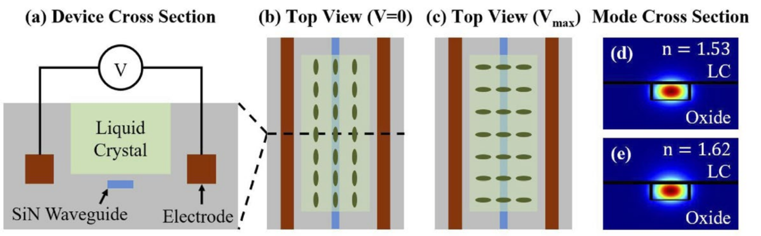

(a) Simplified cross-sectional diagram of the liquid-crystal-based phase modulator consisting of a silicon-nitride waveguide recessed within silicon dioxide below a liquid-crystal-filled trench with integrated electrodes on each side (not to scale). (b) Simplified top-view schematic of the device when no voltage is applied across the liquid-crystal region, resulting in parallel alignment of the liquid-crystal molecules with respect to the waveguide (not to scale). (c) Simplified top-view schematic of the device when the maximum voltage is applied across the liquid-crystal region, resulting in complete rotation of the liquid-crystal molecules and perpendicular alignment of the molecules with respect to the waveguide (not to scale). Simulated mode profiles of the fundamental transverse-electric mode supported by the device (d) at the low liquid-crystal index of n=1.53n=1.53 and (e) at the high liquid-crystal index of n=1.62n=1.62.

KEVIN P. O'BRIEN, *EECS*

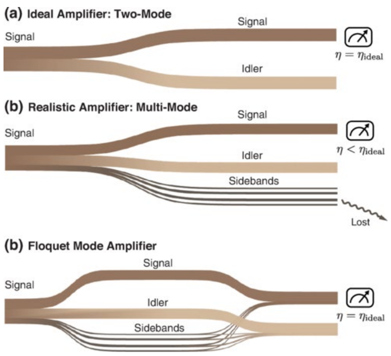

"Floquet-Mode Traveling-Wave Parametric Amplifiers"
Kaidong Peng, Mahdi Naghiloo, Jennifer Wang, Gregory D. Cunningham, Yufeng Ye, and Kevin P. O'Brien
PRXQuantum.3.020306 (2022) | arXiv:2104.08269 (2021)

A schematic illustration of the information flow in different types of parametric amplifiers. (a) Ideal two-mode amplifiers preserve information perfectly, albeit halving the measurement strength as required by the uncertainty principle. (b) Realistic TWPAs are multimode and a portion of the information leaks into the unmeasured sidebands. (c) Floquet-mode TWPAs, proposed in this work, can coherently recover the leaked information back into the signal and idler and reach quantum-limited performance, despite their multimode behavior.






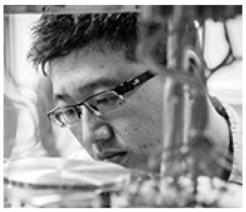

WILLIAM D. OLIVER, *EECS, Physics, Lincoln Laboratory*

with Jeff Grover, RLE; Simon Gustavsson, RLE; Terry Orlando, EECS; Mollie Schwartz, Lincoln Laboratory; Joel I-Jan Wang, RLE; Jonilyn Yoder, Lincoln Laboratory

“Demonstration of tunable three-body interactions between superconducting qubits”
T. Menke, W. P. Banner, T. R. Bergamaschi, A. Di Paolo, A. Vepsäläinen, S. J. Weber, R. Winik, A. Melville, B. M. Niedzielski, D. Rosenberg, K. Serniak, M. E. Schwartz, J. L. Yoder, A. Aspuru-Guzik, S. Gustavsson, J. A. Grover, C. F. Hirjibehedin, A. J. Kerman, W. D. Oliver
arXiv:2205.04542 (2022)

“Extensible circuit-QED architecture via amplitude- and frequency-variable microwaves”
A. Di Paolo, C. Leroux, T. M. Hazard, K. Serniak, S. Gustavsson, A. Blais, W. D. Oliver
arXiv:2204.08098 (2022)

“On-demand directional photon emission using waveguide quantum electrodynamics”
B. Kannan, A. Almanakly, Y. Sung, A. Di Paolo, D. A. Rower, J. Braumüller, A. Melville, B. M. Niedzielski, A. Karamlou, K. Serniak, A. Vepsäläinen, M. E. Schwartz, J. L. Yoder, R. Winik, J. I-Jan Wang, T. P. Orlando, S. Gustavsson, J. A. Grover, W. D. Oliver
arXiv:2203.01430 (2022)

“Mediated interactions beyond the nearest neighbor in an array of superconducting qubits”
Y. Yanay, J. Braumüller, T. P. Orlando, S. Gustavsson, C. Tahan, W. D. Oliver
Phys. Rev. Applied 17, 034060 (2022) | arXiv:2110.01699 (2021)

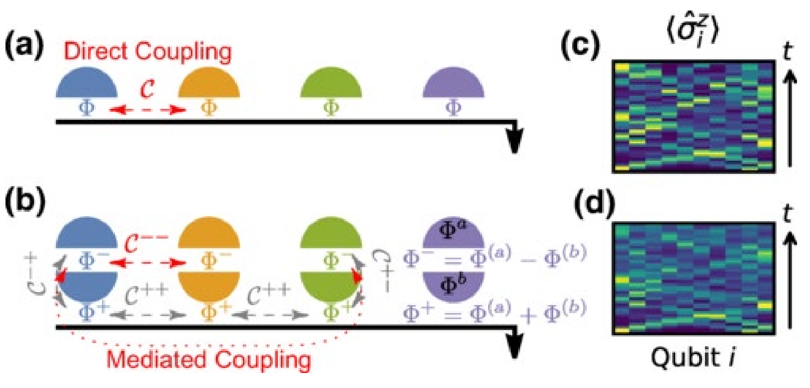

We compare two designs for an array of superconducting qubits. (a) Each “single-ended” qubit is a single superconducting pad, whose phase difference to ground encodes the qubit. Different qubits are coupled by direct capacitance. (b) By contrast, “floating” qubits are made up of a pair of pads each (here shown in the same color), and so have 2 quantum degrees of freedom. The qubit is encoded in the phase difference between the pads, Φ−, and these modes are again coupled to each other by direct capacitance. The average phase to ground, Φ+, does not appear in any inductive element, and can be integrated away. However, because the “+” mode are coupled to the “−” modes and to each other, they mediate an effective interaction, which can extend beyond the nearest neighbor (NN). This


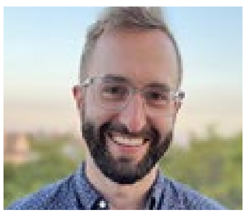



WILLIAM D. OLIVER, *EECS, Physics, Lincoln Laboratory*

with Jeff Grover, RLE; Simon Gustavsson, RLE; Terry Orlando, EECS; Mollie Schwartz, Lincoln Laboratory; Joel I-Jan Wang, RLE; Jonilyn Yoder, Lincoln Laboratory

coupling can fundamentally change the nature of the system; for example, a qubit chain with NN hopping is an integrable system: it retains a memory of its initial state. This is seen in (c), where a chain of ten qubits is initiated with two excitations, and their trajectories can be seen even at long times. By comparison, when the floating qubit array is initiated in the same state in (d), it quickly reaches local equilibrium. See Sec. 4 for more detail.

"Quantum transport and localization in 1d and 2d tight-binding lattices"

A. H. Karamlou, J. Braumüller, Y. Yanay, A. Di Paolo, P. Harrington, B. Kannan, D, Kim, M. Kjaergaard, A. Melville, S. Muschinske, B. Niedzielski, A. Vepsäläinen, R. Winik, J. L. Yoder, M. Schwartz, C. Tahan, T. P. Orlando, S. Gustavsson, W, D. Oliver

npj Quantum Inf 8, 35 (2022) | arXiv:2107.05035 (2021)

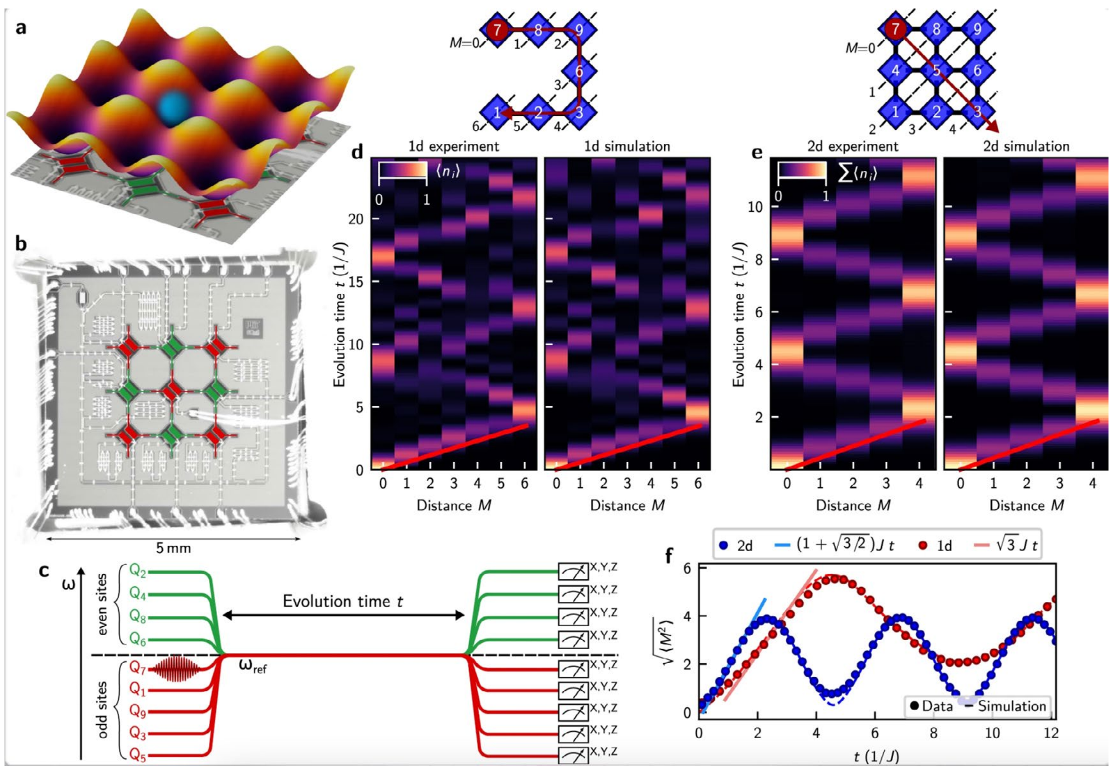

Experimental concept and quantum random walks.

a 2d periodic potential emulated by the superconducting quantum circuit. b Optical image of the 3 × 3 superconducting qubit lattice used in the experiment. The capacitor pads of the transmons qubits are false colored. c Operation sequence of the experiments. Each qubit is initially detuned from ωref and can be addressed individually, and simultaneously. They are brought on resonance to emulate evolution under H^H^ for time t. The system dynamics are frozen by once again detuning the qubits, and all nine qubits are measured simultaneously. d A 1d quantum random walk with a single excitation (particle) initialized at the edge of the lattice (site 7). e A 2d quantum random walk with a single excitation (particle) initialized at the corner of the lattice (site 7). f The spatial propagation of the particle is measured by the root of the second moment of position (⟨M2⟩−−−−−√⟨M2⟩) in the 1d and 2d lattices. The excitation initialized at the edge of the 1d chain exhibits ballistic propagation in time and with propagation speed vg=3–√Jvg=3J (red line), whereas

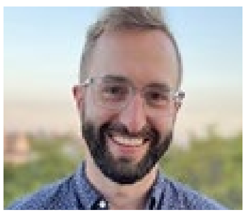

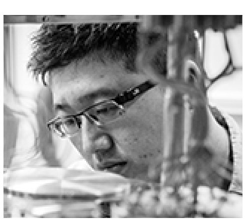

WILLIAM D. OLIVER, *EECS, Physics, Lincoln Laboratory*

with Jeff Grover, RLE; Simon Gustavsson, RLE; Terry Orlando, EECS; Mollie Schwartz, Lincoln Laboratory; Joel I-Jan Wang, RLE; Jonilyn Yoder, Lincoln Laboratory

an excitation initialized in the corner of a 2d lattice exhibits an increased propagation speed vg=(1+3/2−−−√)Jvg=(1+3/2)J (blue line).

"Building a quantum engineering undergraduate program"
A. Asfaw, A. Blais, K. R. Brown, J. Candelaria, C. Cantwell, L. D. Carr, J. Combes, D. M. Debroy, J. M. Donohue, S. E. Economou, E. Edwards, M. F. J. Fox, S. M. Girvin, A. Ho, H. M. Hurst, Z. Jacob, B. R. Johnson, E. Johnston-Halperin, R. Joynt, E. Kapit, J. Klein-Seetharaman, M. Laforest, H. J. Lewandowski, T. W. Lynn, C. R. H. McRae, C. Merzbacher, S. Michalakis, P. Narang, W. D. Oliver, J. Palsberg, D. P. Pappas, M. G. Raymer, D. J. Reilly, M. Saffman, T. A. Searles, J. H. Shapiro, C. Singh
IEEE Transactions on Education (2022) | arXiv:2108.01311 (2021)

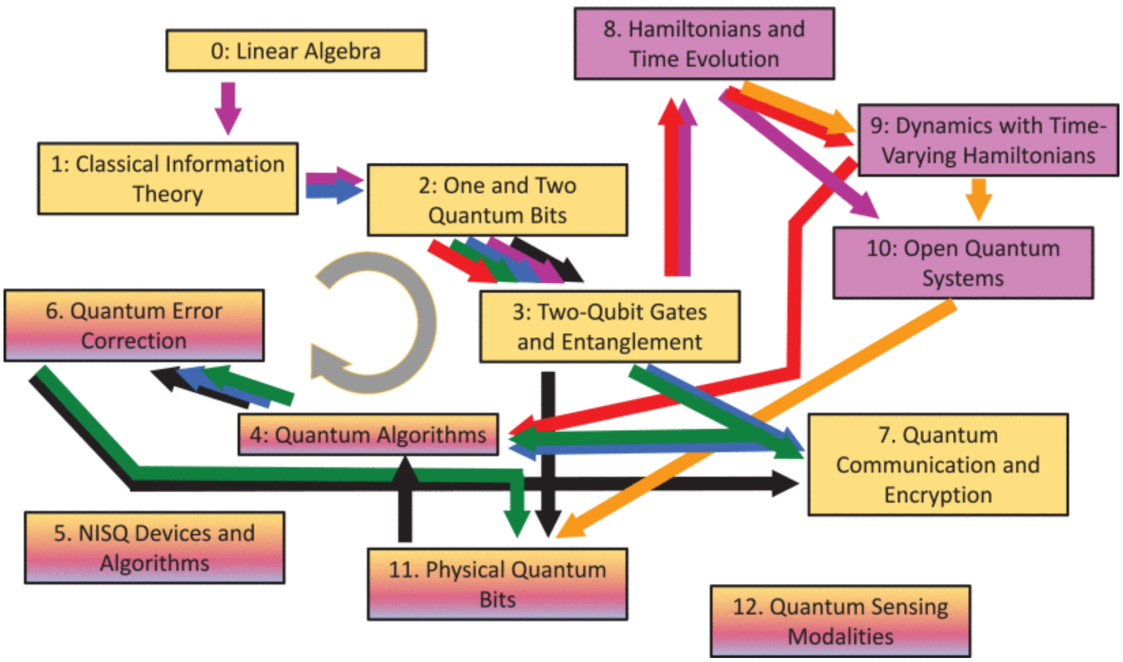

Quantum engineering course modules suggested for STEM students at any level (orange shaded text box), all levels plus advanced students (orange fade to purple), and advanced students only (purple). Arrows between boxes show different sequences taught by the authors (see text), which can be used as a basis for future engineering education research and course development upon formulating program and institution-tailored learning goals (green: Blais; purple: Carr; dark blue (first semester), orange (second semester): Economou; red: Kapit; and black: Lynn). The broad gray circular arrow highlights a particular choice (Girvin) as an example, 1-2-3-4-6. Note that particular connections, such as modules 2 to 3, are almost universal, while some, such as 5 and 12, are presently aspirational.

KYLE SERNIAK, *Lincoln Laboratory*

[“Distinguishing parity-switching mechanisms in a superconducting qubit”]
Spencer Diamond, Valla Fatemi, Max Hays, Kyle Serniak, et. al
arXiv:2204.07458 (2022)

“Superconducting qubits as musical synthesizers for live performance”
Spencer Topel, Kyle Serniak, Luke Burkhart, Florian Carle
arXiv:2203.07879 (2022)

“Superconducting-semiconducting voltage-tunable qubits in the third dimension”
Thomas M. Hazard, Andrew J. Kerman, Kyle Serniak, Charles Tahan
arXiv:2203.06209 (2022)

JEFFREY H. SHAPIRO, *EECS*

“Demonstration of quantum-limited discrimination of multi-copy pure versus mixed states”
Arunkumar Jagannathan, Olivia Brasher, Michael Grace, Jeffrey H. Shapiro, Saikat Guha, Jonathan L. Habif
Phys. Rev. A 105, 032446 (2022) | arXiv:2111.14890 (2021)

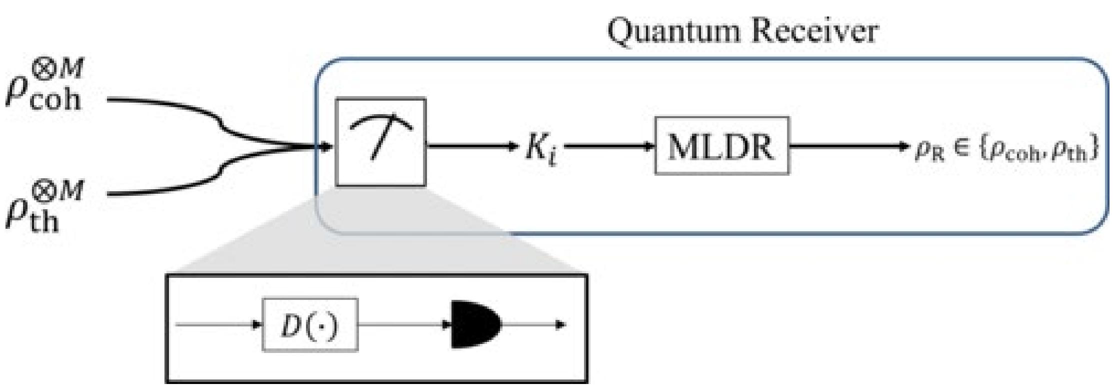

Schematic of multicopy quantum discrimination. Two multicopy sources are equally likely to illuminate the receiver. Copy-by-copy quantum measurements are made on the M arriving states, and the measurement results (Ki) are employed in a maximum-likelihood decision rule (MLDR) to decide which source was present.

VIVISHEK SUDHIR, *ME*

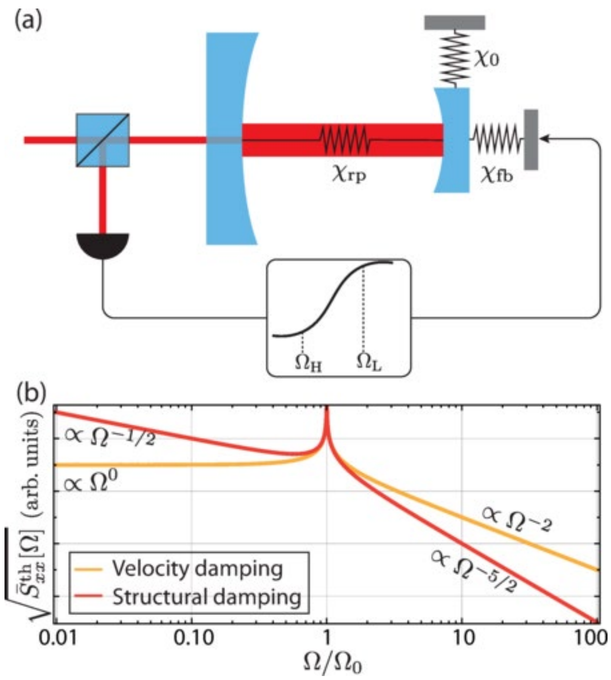

[“Quantum theory of feedback cooling of an anelastic macro-mechanical oscillator”]

Kentaro Komori, Dominika Ďurovčíková, Vivishek Sudhir
Phys. Rev. A 105, 043520 (2022) | arXiv:2111.02412 (2021)

(a) A schematic picture of our model of feedback cooling. A mechanical oscillator with intrinsic susceptibility χ0 is trapped by two additional springs—one induced by optical radiation pressure (χrp) and another induced by measurement-based feedback (χfb)—so that the effective resonant frequency is significantly increased. The feedback filter is characterized by two cutoff frequencies ΩH,L that define the mechanical mode of interest.
(b) Displacement fluctuations of a structurally damped (red) and velocity-damped (yellow) oscillator, showing the stronger decrease of structural thermal noise at frequencies above resonance.

TIMOTHY SWAGER, *Chemistry*

“Dynamic Polypyrrole Core–Shell Chemomechanical Actuators”

Weize Yuan, Harikrishnan Vijayamohanan, Shao-Xiong Lennon Luo, Keith Husted, Jeremiah A. Johnson, and Timothy M. Swager
Chem. Mater., 34, 7, 3013–3019 (2022)

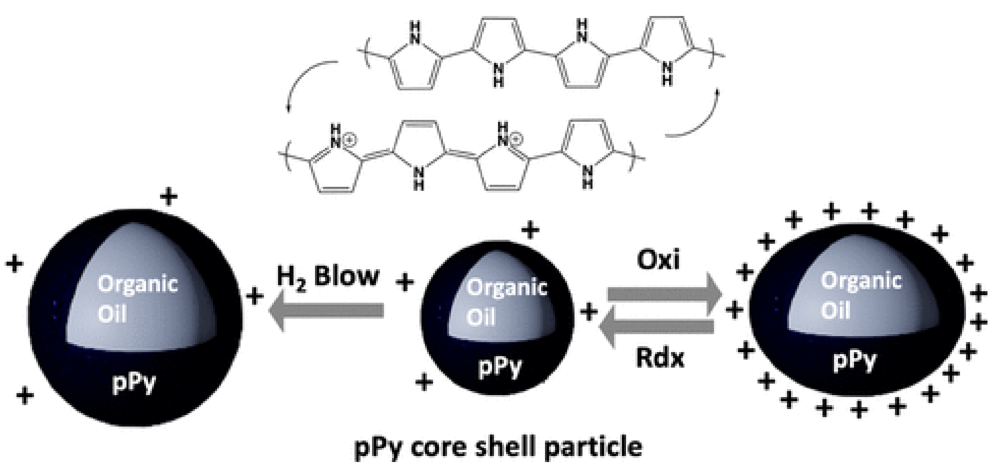

TIMOTHY SWAGER, *Chemistry*

“Multifunctional Photonic Janus Particles”

Qilin He, Harikrishnan Vijayamohanan, Jie Li, and Timothy M. Swager
Journal of the American Chemical Society 144 (12), 5661-5667 (2022)

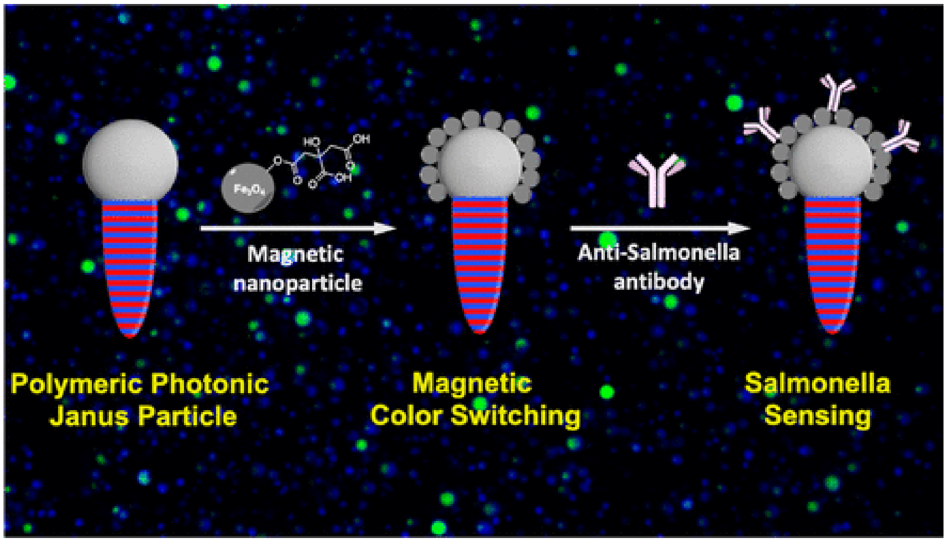

“A Microporous Poly(arylene ether) Platform for Membrane-Based Gas Separation”

Sheng Guo, Jingying Yeo,Francesco Benedetti, Duha Syar, Timothy Swager, Zachary Smith
chemRxiv (2022)

“Solution-processable microporous polymer platform for heterogenization of diverse photoredox catalysts”

Richard Y. Liu, Sheng Guo, Shao-Xiong Lennon Luo and Timothy M. Swager
Nature Communications 13 (1), 1-8 (2022)

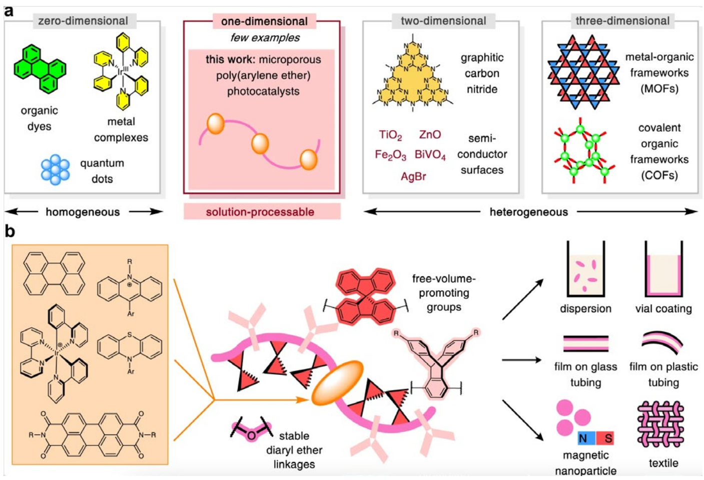

a Classification of photoredox catalysts according to solubility and geometric dimension of active surface. b Transforming a broad scope of small-molecule photocatalysts into diverse heterogeneous materials through solution-processable polymers.

SENTHIL TODRARI, *Physics*

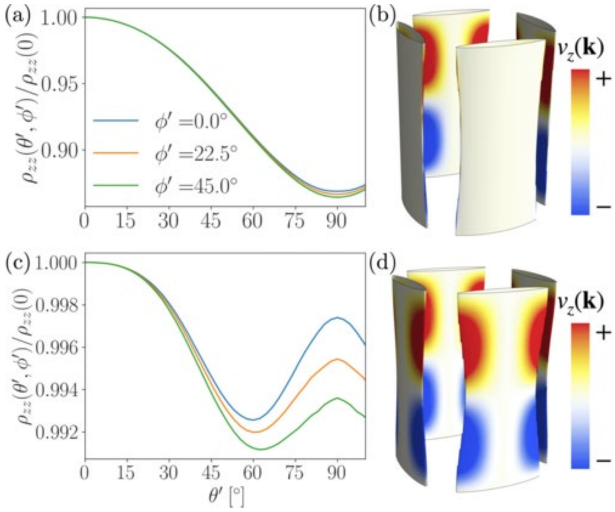

[“Interpreting Angle Dependent Magnetoresistance in Layered Materials: Application to Cuprates”]

Seth Musser, Debanjan Chowdhury, Patrick A. Lee, T. Senthil
Phys. Rev. B 105, 125105 (2022) | arXiv:2111.08740 (2021)

ADMR curves for normalized c-axis resistivity: (a) including the momentum-dependent Zk, due to a (π,π) SDW reconstruction at p=0.21. The parameters are otherwise the same as those used in [10]; (c) setting Zk=1 in the presence of the same SDW. This reproduces the results in [10]. The electron spectral function and hole pockets: (b) including the nontrivial Zk. The colors represent the value of vz(k) on the Fermi surface. The backside of the hole pockets are white since Zk→0; (d) setting Zk=1. The backside of the hole pockets have an artificial nonzero spectral weight and a finite vz(k).

“Lowest Landau level theory of the bosonic Jain states”

Hart Goldman, T. Senthil
Phys. Rev. B 105, 075130 (2022) | arXiv:2110.03700 (2021)

A schematic of the emergence of the bosonic Jain states. Our starting point is a theory of bosons in a magnetic field with interaction energy, Vint, and cyclotron frequency, ωc. The bosons are projected to the lowest Landau level (LLL) when Vint≪ωc (we use units ħ=c=1). By changing variables to composite fermions c, coupled to a fluctuating gauge field aμ, we consider a composite Fermi liquid (CFL) theory on the noncommutative space of the LLL, which is valid below the interaction scale. We access the Jain states by turning on a background vector potential δAi, such that the composite fermions fill p Landau levels with a gap Δp. Integrating out the composite fermions leads to an effective noncommutative Chern-Simons theory, which captures the topological data of the Jain state.

“Pairing symmetry of twisted bilayer graphene: a phenomenological synthesis”

Ethan Lake, Adarsh S. Patri, T. Senthil
arXiv:2204.12579 (2022)

“Continuous Mott transition in moiré semiconductors: role of long-wavelength inhomogeneities”

Sunghoon Kim, T. Senthil, Debanjan Chowdhury
arXiv:2204.10865 (2022)

SENTHIL TODRARI, *Physics*

"Gifts from anomalies: Exact results for Landau phase transitions in metals"
Zhengyan Darius Shi, Hart Goldman, Dominic V. Else, T. Senthil
arXiv:2204.07585 (2022)

"Evolution between quantum Hall and conducting phases: simple models and some results"
Zhihuan Dong, T. Senthil
Phys. Rev. B 105, 085301 (2022) | arXiv:2107.06911 (2021)

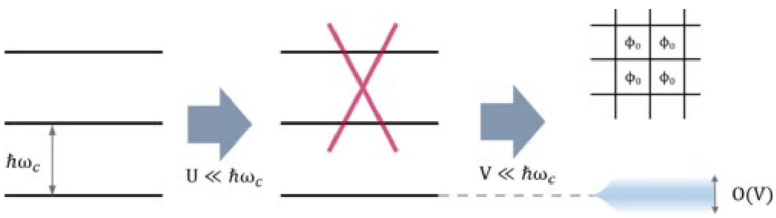

Projection to LLL and the effect of a periodic potential. ωc is the cyclotron frequency. U denotes the interparticle interaction and V the strength of a periodic potential whose unit cell encloses exactly one flux quantum ϕ0.

TROY VAN VOORHIS, *Chemistry*

"Diabatic Valence-Hole States in the C2 Molecule: "Putting Humpty Dumpty Together Again"
Jun Jiang, Hong-Zhou Ye, Klaas Nauta, Troy Van Voorhis, Timothy W. Schmidt, and Robert W. Field
J. Phys. Chem. A, 126, 20, 3090–3100 (2022) | arXiv:2203.03138 (2022)

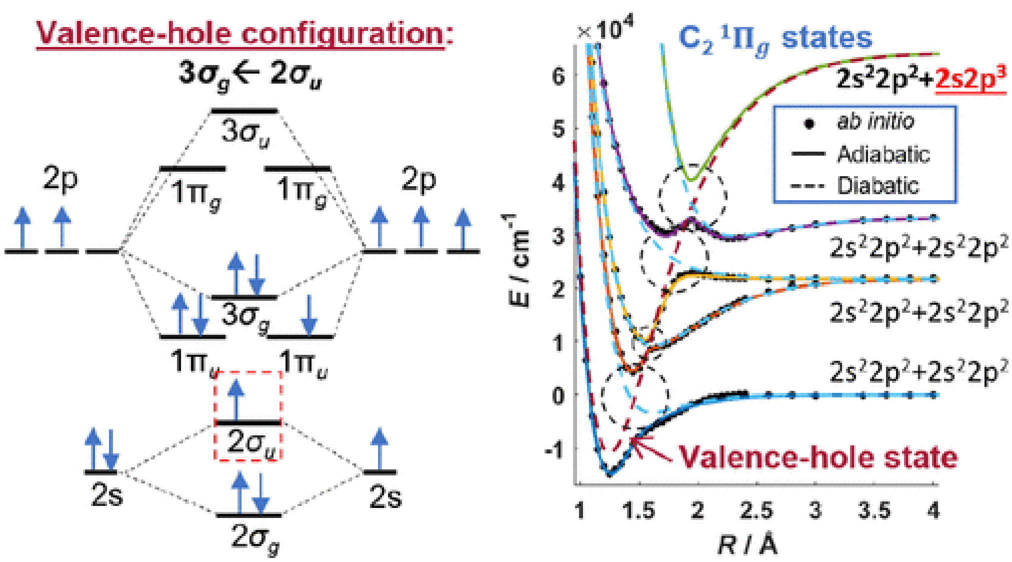

VLADAN VULETIC, *Physics*

“Evidence of Two-Source King Plot Nonlinearity in Spectroscopic Search for New Boson”

Joonseok Hur, Diana P. L. Aude Craik, Eugene Knyazev, Ian Counts, Luke Caldwell, Calvin Leung, Swadha Pandey, Julian C. Berengut, Amy Geddes, Witold Nazarewicz, Paul-Gerhard Reinhard, Akio Kawasaki, Honggi Jeon, Wonho Jhe, Vladan Vuletić

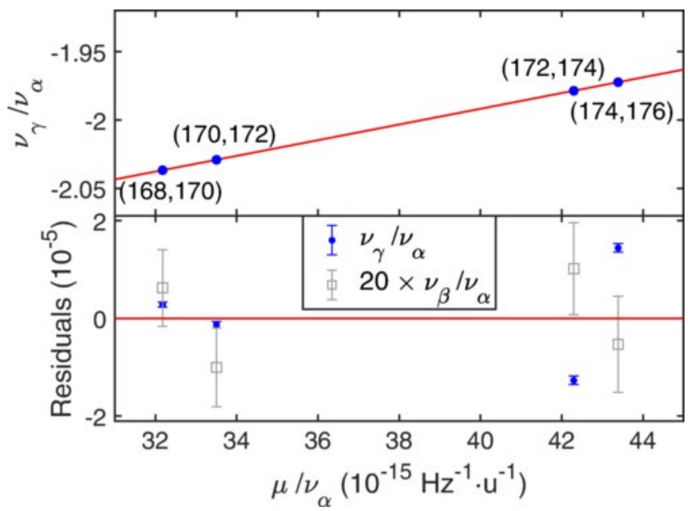

Phys. Rev. Lett. 128, 163201 (2022) | arXiv:2201.03578 (2022)

Frequency-normalized King plot (top) and residuals (bottom, blue) for the γ (2S1/2→2F7/2) transition and reference transition α (2S1/2→2D5/2) for even-neighbor pairs (A′=A+2) of Yb+ isotopes. A deviation from linearity (red line) by 41 standard deviations σ is observed. For reference, residuals for the β (2S1/2→2D3/2) transition [19], magnified 20-fold, are also plotted in gray. The error bars indicate 2σ uncertainties; for correlations between the errors, see Supplemental Material [24].

“A quantum processor based on coherent transport of entangled atom arrays”

Dolev Bluvstein, Harry Levine, Giulia Semeghini, Tout T. Wang, Sepehr Ebadi, Marcin Kalinowski, Alexander Keesling, Nishad Maskara, Hannes Pichler, Markus Greiner, Vladan Vuletic, Mikhail D. Lukin

Nature volume 604, pages451–456 (2022)| arXiv:2112.03923 (2021)

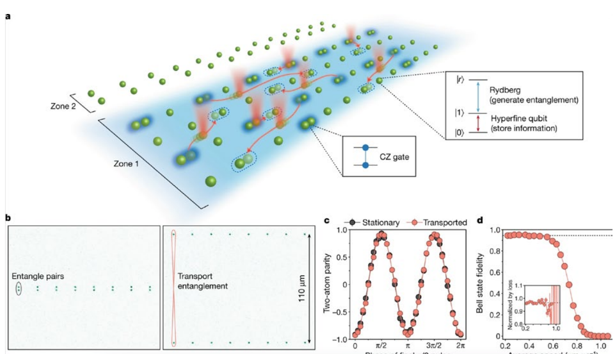

a, In our approach, qubits are transported to perform entangling gates with distant qubits, enabling programmable and non-local connectivity. Atom shuttling is performed using optical tweezers, with high parallelism in two dimensions and between multiple zones allowing selective manipulations. Inset: the atomic levels used. The |0⟩, |1⟩ qubit states refer to the mF = 0 clock states of 87Rb, and |r⟩ is a Rydberg state used for generating entanglement between qubits (Extended Data Fig. 1b). b, Atom images illustrating coherent transport of entangled qubits. Using a sequence of single-qubit and two-qubit gates, atom pairs are each prepared in the |Φ+⟩ Bell state (Methods), and are then separated by 110 µm over a span of 300 µs. c, Parity oscillations indicate that movement does not observably affect entanglement or coherence. For both the moving and the stationary measurements, qubit coherence is preserved using an XY8 dynamical decoupling sequence for 300 µs (Methods). d, Measured Bell-state fidelity as a function of separation speed over the 110 µm, showing that fidelity is unaffected for a move slower than 200 µs (average separation speed of 0.55 µm µs−1). Inset: normalizing by atom loss during the move results in constant fidelity, indicating that atom loss is the dominant error mechanism (see Methods for details).

VLADAN VULETIC, *Physics*

[“Dispersive optical systems for scalable Raman driving of hyperfine qubits”]

Harry Levine, Dolev Bluvstein, Alexander Keesling, Tout T. Wang, Sepehr Ebadi, Giulia Semeghini, Ahmed Omran, Markus Greiner, Vladan Vuletić, Mikhail D. Lukin

Phys. Rev. A 105, 032618 (2022) | arXiv:2110.14645 (2021)

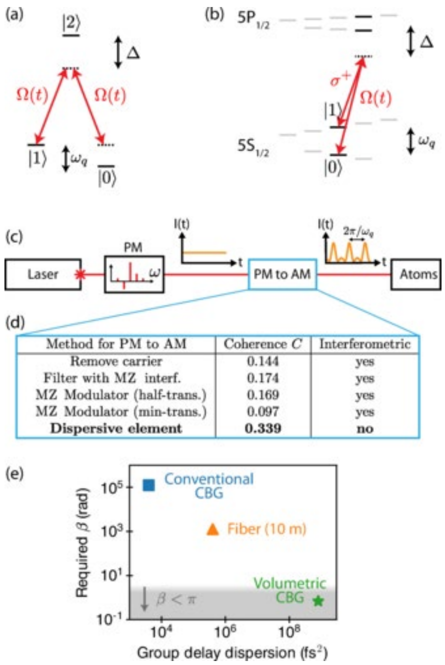

Amplitude modulation for driving Raman transitions. (a) Stimulated Raman transitions in a Λ-type three-level system. Adiabatic elimination of the excited state results in an effective Raman coupling between ground states |0⟩ and |1⟩. (b) Level structure for 87Rb, showing Raman driving of the clock transition from |0⟩=|F=1,mF=0⟩ to |1⟩=|F=2,mF=0⟩. This transition is driven by a time-dependent σ+ polarized field Ω(t), which is far detuned by Δ from the excited state (but not far detuned relative to the splitting between the 5P1/2 and 5P3/2 excited states). (c) Several approaches for Raman driving, including the dispersive approach presented here, operate by converting phase modulation to amplitude modulation at the qubit frequency, which resonantly drives the Raman transition. (d) Comparison of methods for converting phase modulation to amplitude modulation. The dispersive approach benefits both from having the highest coherence metric (see Appendix pp2) and from being passively stable since it does not rely on interferometric filtering. (e) Weakly dispersive elements, such as a conventional chirped Bragg mirror or a 10-m optical fiber, require large modulation depth β to achieve efficient amplitude modulation, according to Eq. (7). The highly dispersive volumetric CBG allows a low β to be used. Here β≲π marks the experimentally accessible window of modulation depths.

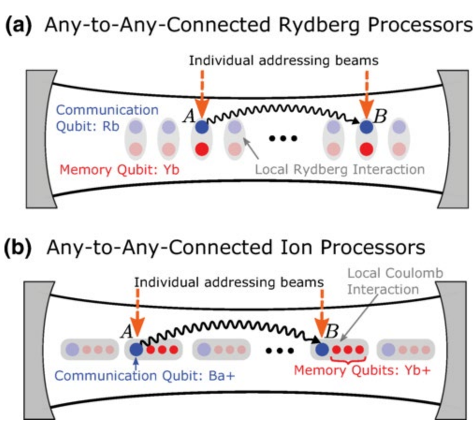

“Any-to-any connected cavity-mediated architecture for quantum computing with trapped ions or Rydberg arrays”

Joshua Ramette, Josiah Sinclair, Zachary Vendeiro, Alyssa Rudelis, Marko Cetina, Vladan Vuletić

PRX Quantum 3, 010344 (2022) | arXiv:2109.11551 (2021)

Architecture for cavity-mediated quantum gate between any two qubits applied to (a) Rydberg atoms or (b) multiple chains of trapped ions. Photon transfers via the cavity produce heralded entanglement of communication qubits. Local interactions between communication and memory qubits enable teleported gates between any two memory qubits. Different atomic species can be used for the communication and memory qubits so that the latter remain unaffected during the entanglement process for communication qubits.

“Machine-learning-accelerated Bose-Einstein condensation”

Zachary Vendeiro, Joshua Ramette, Alyssa Rudelis, Michelle Chong, Josiah Sinclair, Luke Stewart, Alban Urvoy, Vladan Vuletić

arXiv:2205.08057 (2022)

VLADAN VULETIC, *Physics*

[“Controlling Single Photons with Rydberg Superatoms”]
Wenchao Xu and Vladan Vuletić
Physics (2022)

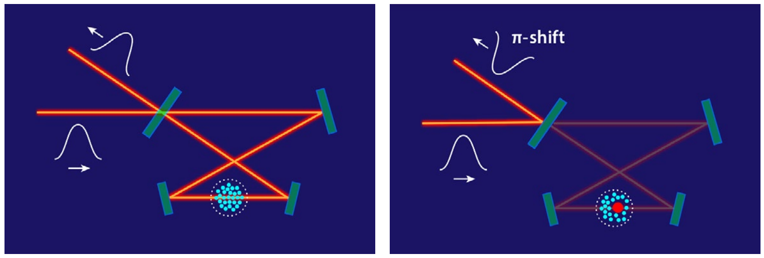

Sketch of the superatom-cavity scheme for photon manipulation. (Top) If the superatom is in its ground state, photons pass through the cavity. (Bottom) If the superatom is in its excited state, photons are reflected at the cavity’s entrance port, and their optical phase is shifted by ππ. The phase shift can be controlled by creating a Rydberg excitation (red dot) in the atomic cloud.

“Quantum optimization of maximum independent set using Rydberg atom arrays”
S. Ebadi, Alexander Keesling, Madelyn Cain,..., Vladan Vuletic, Mikhail D. Lukin
Science | arXiv:2202.09372

“Collective Spin-Light and Light-Mediated Spin-Spin Interactions in an Optical Cavity”
Zeyang Li, Boris Braverman, Simone Colombo, Chi Shu, Akio Kawasaki, Albert F. Adiyatullin, Edwin Pedrozo-Peñafiel, Enrique Mendez, and Vladan Vuletić
PRX Quantum (2022) | arXiv:2106.13234 (2021)

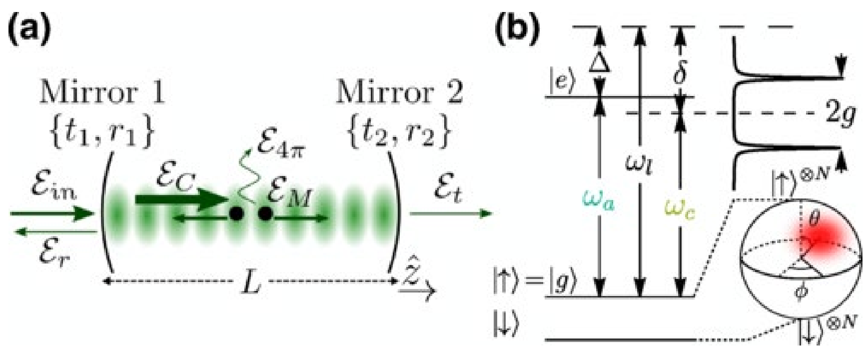

(a) Schematic diagram of an ensemble of atoms interacting with a single-mode cavity of length L. The incident field Ein builds up in the cavity to the value Ec. The cavity field is coherently scattered by the atoms into the cavity with amplitude EM, and coherently radiated through the cavity mirrors to give the transmitted and reflected fields Et and Er. The cavity field scatters from the atoms into free space with amplitude E4π, and from the cavity mirrors with amplitude Esc, which is assumed to be zero in a lossless cavity. (b) Level diagram of the atomic three-level system. Here |↑⟩=|g⟩ and |e⟩ are the two states interacting with the cavity light; ωa,ωc, and ωl are the atomic, cavity resonance frequencies, and the probing light frequency, respectively; Δ=ωl−ωa and δ=ωl−ωc are the detunings of probing light from atomic and cavity resonances, respectively. The curve on the right represents the cavity transmission spectrum in the presence of atoms, and 2g is the vacuum Rabi splitting due to the light-atom interaction when ωa=ωc. The sphere in the bottom right represents a Bloch sphere formed by the N atoms of spin 12, and the shaded distribution represents a coherent spin state (CSS) pointing along polar and azimuthal angles (θ,ϕ) in spherical coordinates where each atom is in a superposition state cos(θ/2)|↑⟩+sin(θ/2)eiϕ|↓⟩.

LINDLEY WINSLOW, *Physics*

"Axion Dark Matter"
J. Jaeckel, G. Rybka, L. Winslow
arXiv:2203.14923 (2022)

"Muon Track Reconstruction in a Segmented Bolometric Array Using Multi-Objective Optimization"
J. Yocum, D. Mayer, J. L. Ouellet, L. Winslow
arXiv:2202.03194 (2022)

Search for Majorana neutrinos exploiting millikelvin cryogenics with CUORE
The CUORE Collaboration, ..., L. Winslow, et. al
Nature volume 604, pages53–58 (2022) | arXiv:2104.06906 (2021)

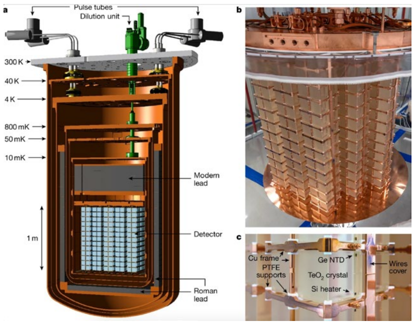

a, Rendering of the six-stage cryostat, with the pulse tubes and dilution unit, the internal low-radioactivity modern and Roman lead shields, and the array of 988 TeO2 crystals (light blue). b, The detector after installation. The plastic ring was used during assembly for radon protection. c, One of the calorimeters instrumented with an NTD Ge thermistor which measures the temperature increase induced by absorbed radiation. The Si heater is used to inject pulses for thermal gain stabilization. The polytetrafluoroethylene (PTFE) supports and the gold wires instrumenting the NTD and the heater provide the thermal link between the crystal and the heat bath, that is, the Cu frames24.

"DMRadio-m3: A Search for the QCD Axion Below 1μeV"
DMRadio Collaboration, ..., L. Winslow, et. al
arXiv:2204.13781 (2022)

"New Horizons: Scalar and Vector Ultralight Dark Matter"
D. Antypas, A. Banerjee, C. Bartram, ..., L. Winslow, et. al
arXiv:2203.14915 (2022)

"Introducing DMRadio-GUT, a search for GUT-scale QCD axions"
L. Brouwer, S. Chaudhuri, H. -M. Cho, ..., L. Winslow, et. al
arXiv:2203.11246 (2022)

Search for neutrinoless β+EC decay of 120Te with CUORE
D. Q. Adams et al. (CUORE Collaboration)
Phys. Rev. C 105, 065504 (2022) | arXiv:2203.08684 (2022)

Determining gA/gV with High Resolution Spectral Measurements Using an LiInSe2 Bolometer
A.F. Leder, D. Mayer, J.L. Ouellet, ..., L. Winslow, et. al
arXiv:2206.06559 (2022)

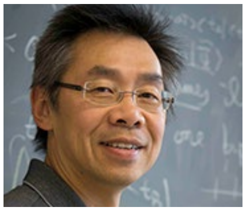

FRANCO N. C. WONG, *RLE*

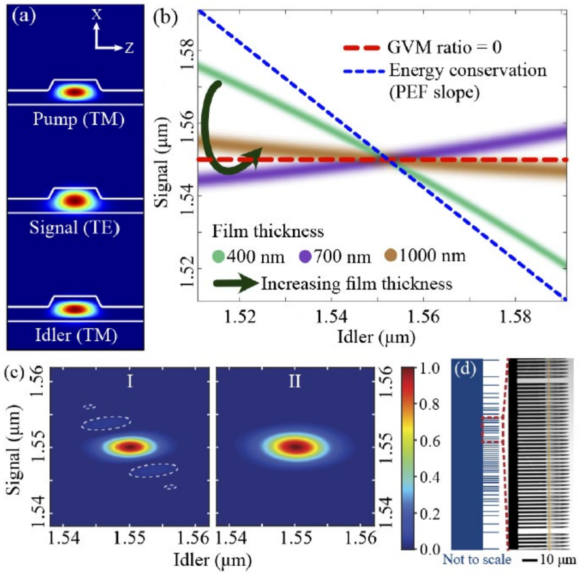

["Spectrally separable photon-pair generation in dispersion engineered thin-film lithium niobite"]
C. J. Xin, Jatadhari Mishra, Changchen Chen, Di Zhu, Amirhassan Shams-Ansari, Carsten Langrock, Neil Sinclair, Franco N. C. Wong, M. M. Fejer, and Marko Lončar
Optica (2022) | arXiv:2202.12469 (2022)

Device design. (a)Normalized cross sectional mode intensities of the pump at 775-nm wavelength and both signal and idler at 1550-nm wavelength. TFLN is outlined in white with air on top and silica cladding underneath, with nominal waveguide dimensions of top width 1200 nm, film thickness 700 nm, etch depth 300 nm, and sidewall angle 62°. (b) Simulated PMF for varied film thickness, other dimensions are the same as above; waveguide length 5 mm. The lines representing zero GVM ratio and slope of the PEF are represented by red and blue dashed lines, respectively. (c) Simulated normalized JSIs for waveguide geometry in panel (a) given by the overlap of Gaussian pumps of FWHMs 0.8 THz and 1.0 THz, and simulated PMFs for (I) non-apodized QPM grating (resulting in a sinc PMF; dashed outline around sidelobes for emphasis) and (II) Gaussian-apodized QPM grating (resulting in a Gaussian PMF), respectively, thus optimizing the respective Pspectral to 90.5%and 99.8%. (d) Deleted-domain Gaussian-apodized poling electrode pattern (left). Two-photon microscopy image of the poled film (right); overlaid yellow line represents the waveguide while black and gray regions show the electrodes and inverted domains, respectively.

"Search for Spatial Correlations of Neutrinos with Ultra-High-Energy Cosmic Rays"
The ANTARES collaboration, ..., Franco N. C. Wong, et al
arXiv:2201.07313 (2022)

BILGE YILDIZ, *NSE MSE*

“Strain-Dependent Surface Defect Equilibria of Mixed Ionic-Electronic Conducting Perovskites”
Jiayue Wang, Jing Yang, Alexander Karl Opitz, Dmitri Kalaev, Andreas Nenning, Ethan J. Crumlin, Jerzy T. Sadowski, Iradwikanari Waluyo, Adrian Hunt, Harry L. Tuller, Bilge Yildiz
Chem. Mater. (2022)

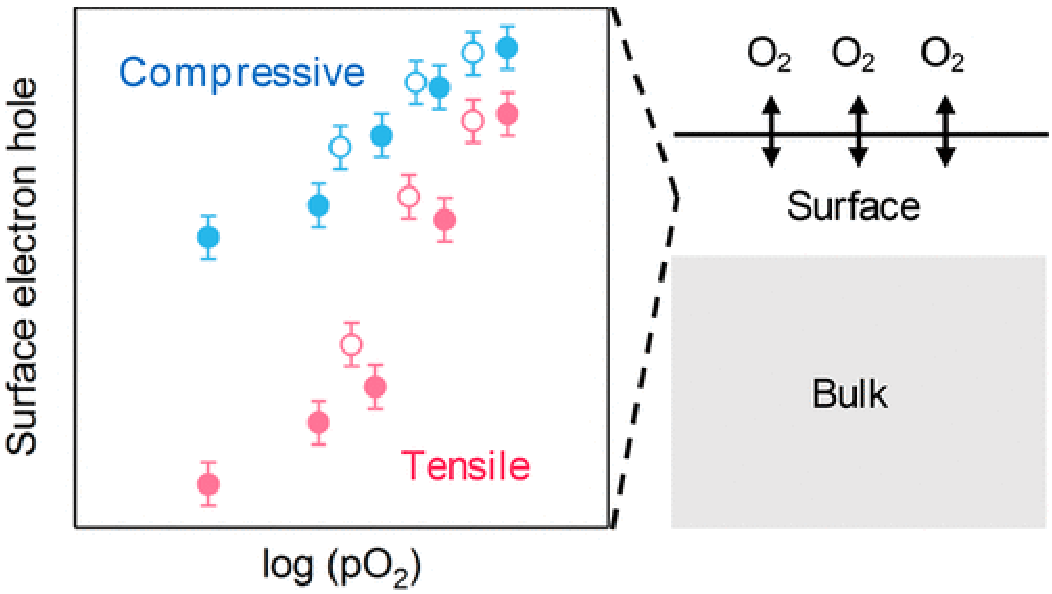

“Thermally-driven reactivity of Li0.35La0.55TiO3 solid electrolyte with LiCoO2 cathode”
Subhash Chandra, Younggyu Kim, Daniele Vivona, Iradwikanari Waluyo, Adrian Hunt, Christoph Schlueter, Jeong Beom Lee, Yang Shao-Horn and Bilge Yildiz
Journal of Materials Chemistry A, 10, 3485-3494 (2022)

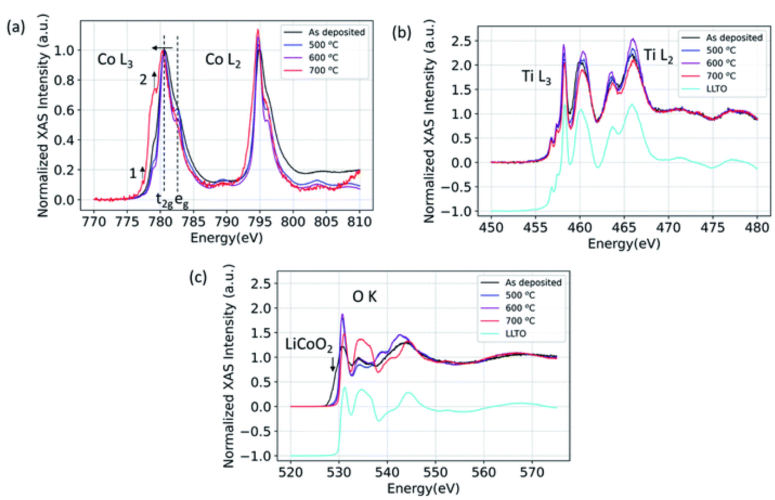

(a) Co L3 and Co L2, (b) Ti L3 and Ti L2, (c) O K X-ray absorption spectra for 100 nm LCO|LLTO for the as-deposited sample and for samples annealed at different temperatures in air.

BILGE YILDIZ, *NSE MSE*

“Thermally Controlled Activation and Passivation of Surface Chemistry and Oxygen-Exchange Kinetics on a Perovskite Oxide”

Đorđije Tripković, Jiayue Wang, Rainer Küngas, Mogens Bjerg Mogensen, Bilge Yildiz, and Peter Vang Hendriksen

Chemistry of Materials, 2022, 34, 4, 1722–1736. (2022)

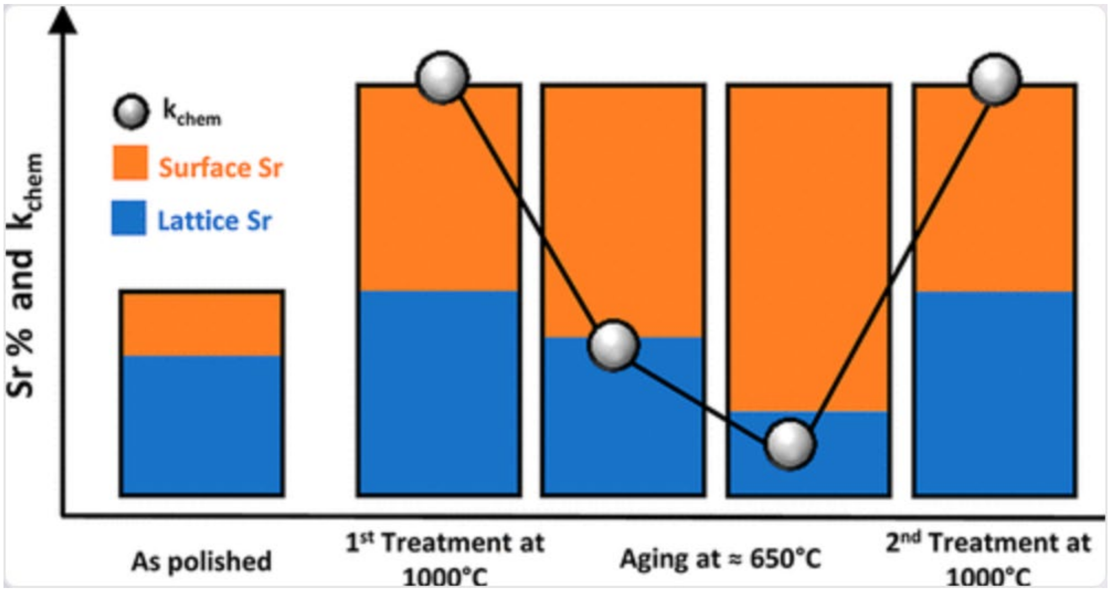

“Avoiding CO2 improves thermal stability at the interface of Li7La3Zr2O12 Electrolyte with Layered Oxide Cathodes”

Younggyu Kim, Iradwikanari Waluyo, Adrian Hunt, and Bilge Yildiz

Advanced Energy Materials, 2102741 (2022)

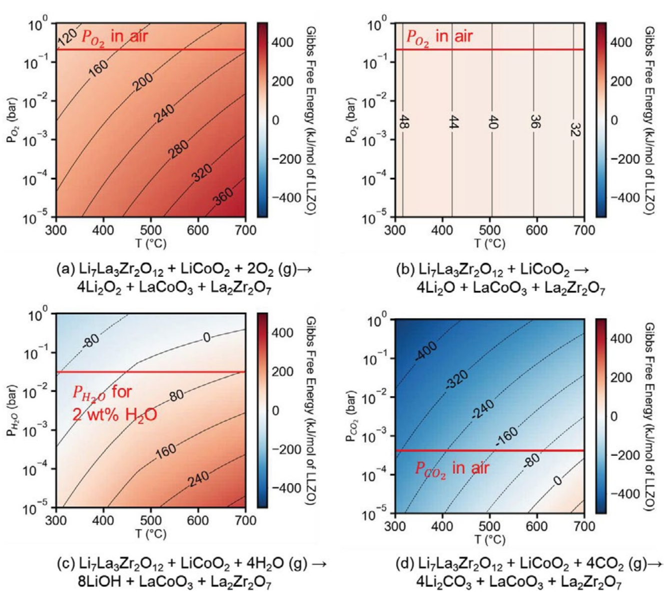

The Gibbs free energy, ΔG(T,Pgas) (kJ mol–1 of LLZO) calculated between LLZO and fully lithiated LiCoO2 in a) Li7La3Zr2O12 + LiCoO2 + 2O2(g) → 4Li2O2 + LaCoO3 + La2Zr2O7, b) Li7La3Zr2O12 + LiCoO2 → 4Li2O + LaCoO3 + La2Zr2O7, c) Li7La3Zr2O

MARTIN ZWIERLEIN, *Physics*

“Resonant and first-order dipolar interactions between ultracold $^1\Sigma$ molecules in static and microwave electric fields”
Tijs Karman, Zoe Z. Yan, and Martin Zwierlein
Phys. Rev. A 105, 013321 (2022) | arXiv:2106.01610 (2021)

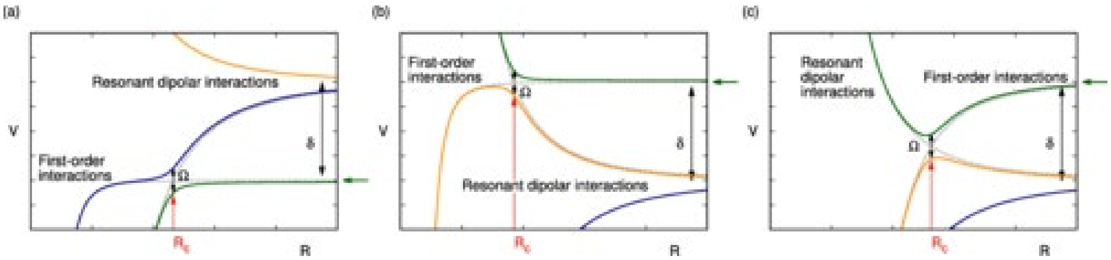

Illustration of the competition of first-order and resonant dipolar interactions explored in this work. Dashed lines indicate diabatic field-dressed interaction potentials, which cross at the Condon point marked Rc, whereas the solid lines indicate adiabatic potentials for which the crossing is avoided due to the Rabi coupling. Panel (a) sketches the interaction potentials for a pair of resonantly interacting states occurring above the initial state (in green, indicated by an arrow), as is realizable by dressing with microwaves red detuned from a rotational transition. In the illustration, the attractive branch of the resonant dipolar interaction [in blue (dark gray)] crosses the ground-state interaction potential outside the range of first-order dipolar interactions, where coupling between these potentials can transform the dynamics qualitatively. Panel (b) shows dressing with blue detuning gives access to resonantly interacting states below the initial state, such that the repulsive branch of the resonant dipolar interaction [in orange (light gray)] crosses the initial potential. Repulsive resonant dipolar interactions can reduce short-range loss rates by orders of magnitude even if the interactions become repulsive only at shorter range, as shown in panel (c). The combination of long-range first-order dipolar interactions and repulsive resonant dipolar interactions at shorter range can support quasibound states and lead to scattering resonances.

“Photons think inside the box”
Richard J. Fletcher and Martin Zwierlein
Science (2022)

Publications

Quantum optimization of maximum independent set using Rydberg atom arrays
S. Ebadi, et. al., including MIT-CQE member, E. Farhi [Science]

Noise-resilient Majorana Edge Modes on a Chain of Superconducting Qubits
X. Mi, et. al., including MIT-CQE member, E. Farhi [arxiv]

Direct measurement of nonlocal interactions in the many-body localized phase
B. Chiaro, et. al., including MIT-CQE member, E. Farhi [Phys. Rev. Research]

Time-crystalline eigenstate order on a quantum processor
X. Mi, et. al., including MIT-CQE member, E. Farhi [Nature]

Quantum advantage in learning from experiments
A classical machine learning system would not be able to directly access and learn from quantum information, the researchers says, whereas the quantum learning agent can access and directly interact with the quantum data, providing a level of analysis not possible in any other way. [Science]

Harvard and QuEra Collaborators Observe Quantum Speed-Up in Optimization Problems
The calculations were performed on Harvard's quantum processor of 289 qubits operating in the analog mode, with effective circuit depths up to 32. Unlike in previous examples of quantum optimization, the large system size and circuit depth used in this work made it impossible to use classical simulations to pre-optimize the control parameters. [arxiv]

The realization of measurement induced quantum phases on a trapped-ion quantum computer
"By starting in a mixed state with high entropy, or information, then evolving the circuits, the entropy at the end of the circuit indicates whether that information has been lost, or in other words the system has purified," Noel explained. [nature physics]

Quantum machine Borealis achieves computational advantage using programmable photonic sensor
The researchers took on the boson sampling challenge using a photonic machine that uses photons to represent qubits. Technically called the Gaussian boson sampling challenge, it involves preparing states of light and directing them through a network of beam splitters and then counting how many of the photons arrive at a detector. [Nature]

Quantum machine Borealis achieves computational advantage using programmable photonic sensor
The researchers took on the boson sampling challenge using a photonic machine that uses photons to represent qubits. Technically called the Gaussian boson sampling challenge, it involves preparing states of light and directing them through a network of beam splitters and then counting

how many of the photons arrive at a detector. [Nature]

Doubling up Cooper pairs to protect qubits in quantum computers from noise
The researchers came up with a new kind of superconducting qubit in which the quantum states are nonlocalized by modifying the Josephson junction. In their setup, two Cooper pairs were allowed to tunnel through simultaneously. [PRX]

Fundamental Breakthrough: Error-Free Quantum Computing Gets Real
The physicists have now demonstrated all the building blocks for fault-tolerant computing on a quantum computer. The task now is to implement these methods on larger and hence more useful quantum computers. [arxiv]

Teleportation breakthrough paves the way for quantum internet
Hanson says: "Regarding quantum communication, our work shows how teleportation can be used in a real network environment, with nodes that have no direct connection. In a future quantum internet, such teleportation will be the main way to transfer quantum information over large distances." [Nature]

Diamond qubits are fault-tolerant
"Because of the long coherence times of our qubits," said project supervisor Tim Taminiau, "we could process the outcomes of the measurements on-the-fly while the processor was running. That said, "there is still a long way to go for large-scale fault-tolerant computation," said fellow supervisor Barbara Terhal. [arxiv]

Building a better quantum bit: New qubit breakthrough could transform quantum computing
The team created its qubit by freezing neon gas into a solid at very low temperatures, spraying electrons from a light bulb onto the solid and trapping a single electron there. [Nature]

Quantum computing needs the right combination of order and disorder
'In our study, we ask just how reliable the "stability by randomness" principle is in practice. By applying state-of-the-art diagnostics of the theory of disordered systems, we were able to find that at least some of the industrially pursued system architectures are dangerously close to instability.' [Nature Communications]

Quantum Future: Developing the Next Generation of Quantum Algorithms and Materials
This work provides a cheaper and faster way to perform quantum error correction. It potentially brings us closer to demonstrating a computationally useful example of a quantum simulation for quantum field theory on near-term quantum hardware," said Wiebe. [arxiv]

A quantum sense for dark matter
"We have to keep these devices very, very well isolated from the environment so that when we see the very, very rare event, we're more confident that it might be due to the dark matter." says Aaron Chou, a physicist at

Fermi National Accelerator Laboratory (Fermilab) who works on ADMX. [Science]

Dynamic compensation of stray electric fields in an ion trap using machine learning and adaptive algorithm
Here we demonstrate the compensation of stray electric fields using a gradient descent algorithm and a machine learning technique, which trained a deep learning network. [Nature]

Advancing materials science for superconducting quantum circuits
By utilizing the inherent high resolution provided by high magnetic field EPR, in combination with nuclear spectroscopy techniques, the team were able to study a specific surface radical on Al2O3 (a material present in all modern superconducting quantum processors) in detail. [Science Advances]

A world-first one-way superconductor could make computers 400 times faster
The team created a so-called "Quantum Material Josephson Junctions" with two superconductors separated by a layer of Nb3Br8. [Nature]

2^{1296} Exponentially Complex Quantum Many-Body Simulation via Scalable Deep Learning Method
We report that a deep learning based simulation protocol can achieve the solution with state-of-the-art precision in the Hilbert space as large as 2^{1296} for spin system and 3^{144} for fermion system. [arxiv]

Lasers trigger magnetism in atomically thin quantum materials
The team worked with ultrathin sheets — each just three layers of atoms thick — of tungsten diselenide and tungsten disulfide. The researchers were studying the exciton properties within the material when they made the surprising discovery that light triggers a key magnetic property within the normally nonmagnetic material. [Nature]

Anomalous Josephson effect appears in a topological insulator
The researchers found that in this [tri-] junction, exotic particles known as Majorana bound states behave differently when an in-plane magnetic field is applied parallel to the two inline single junctions, compared to when it is applied parallel to the third. [Chinese Physics Letters]

'Quantum Hair' May Resolve Stephen Hawking's Black Hole Paradox
Rather than being merely simple objects with a certain mass, speed and rotation, as defined under classical physics' so-called "no-hair theorem", the team's new findings suggest that black holes are actually more complex and 'hairier' than general relativity might imagine. [Phys. Lett. B]

Quantum Organization Collab Reports Achievement for Neutral Atom Quantum Computing
The team is the first in the world to demonstrate quantum algorithms on a programmable gate model cold atom quantum computer. An architecture was used in which individual atoms

are addressed with tightly focused optical beams scanned across a two-dimensional array of qubits. [Nature]

Quantum approximate optimization algorithm can be implemented using Rydberg atoms

"Existing quantum devices can actually do things that we cannot compute with classical computers. The question is only can we harness this computational power that is apparently there," van Bijnen says. [Phys. Rev. Lett.]

Ancient Namibian stone could hold key to future quantum computers

Rydberg polaritons switch continually from light to matter and back again. In Rydberg polaritons, light and matter are like two sides of a coin, and the matter side is what makes polaritons interact with each other. [Nature Materials]

Graphene-hBN breakthrough to spur new LEDs, quantum computing

Hexagonal boron nitride is the world's thinnest insulator while graphene is the thinnest of a class of materials called semimetals, which have highly malleable electrical properties and are important for their role in computers and other electronics. [Advanced Materials]

AI Fuses With Quantum Computing in Promising New Memristor

Spagnolo and his colleagues instead developed a quantum memristor that relies on a stream of photons existing in superpositions where each single photon can travel down two separate paths laser-written onto glass. [Nature Photonics]

Researchers generate high-quality quantum light with modular waveguide device

A multi-institutional team of researchers from Japan describe the waveguide optical parametric amplifier (OPA) module they created for quantum experiments. Combining this device with a specially designed photon detector allowed them to generate a state of light known as Schrödinger cat, which is a superposition of coherent states. [Optics Express]

Quantum Internet Breakthrough – Bell State Analyzer Presents Giant Leap Toward Fully Quantum Internet

With the Bell state analyzer completed, Lukens and colleagues are looking to expand to a complete entanglement swapping experiment, which would be the first of its kind in frequency encoding. [Optica]

Study highlights the possibility of building wave-shape-tolerant qubit gates

"Regardless of what architecture we consider, photons, the quanta of light, will play an important role, since in almost all architectures the mediators between quantum information bits (qubits) are photons." [Phys. Rev. Lett.]

In race to build quantum computing hardware, silicon begins to shine

Princeton physicists used a two-qubit silicon quantum device to achieve an unprecedented level of fidelity. At above 99 percent, this is the highest fidelity thus far achieved for a two-qubit gate in a semiconductor and is on par with the best results achieved by competing technologies. [Science Advances]

Stanford researchers propose cost-effective, optical quantum computer design
The compiler outlined in Bartlett's paper takes an arbitrary quantum circuit and breaks down each gate into photon- or atom-scattering interactions. [Optica]

New algorithm could be quantum leap in search for gravitational waves
The Glasgow team are the first to adapt Grover's algorithm for the purposes of gravitational wave search. In the paper, they demonstrate how they have applied it to gravitational wave searches through software they developed using the Python programming language and Qiskit, a tool for simulating quantum computing processes. [Physical Review Research]

Spooky Action Could Help Boost Quantum Machine Learning
"Trading entanglement for training states could give huge advantages for training certain types of quantum systems," says study coauthor Andrew Sornborger, a physicist at Los Alamos National Laboratory, in New Mexico. [PRL]

Scientists announce first proof of quantum boomerangs and share backstory of Google's time crystal
We have for the first time observed the 'quantum boomerang effect,' a fundamental feature of localized matter whereby a particle launched in any direction should, on average, return to the origin and remain there—like a boomerang," said David Weld, physicist at the University of California Santa Barbara. [PRX]

Europium and light: An innovative platform for quantum computers and communications
Europium molecular crystals represent a major advance, as they have ultra-narrow linewidths. This translates into long-lived quantum states, which were used to demonstrate the storage of a light pulse inside these molecular crystals. [Nature]

A first step towards quantum algorithms: Minimizing the guesswork of a quantum ensemble
"Guesswork is a very basic scientific problem, but there is very little research on quantum guesswork and even less on the algorithmic implications of quantum guesswork. Our paper goes a little way towards filling that gap," concludes Koshiba. [TIT]

Breakthrough in quantum sensing provides new material to make qubits
Bansil and colleagues found that defects in a certain class of materials, specifically two-dimensional transition metal dichalcogenides, contained the atomic properties conducive to make qubits. [Nat Comms]

Politics and Funding

House Armed Services Committee Approves FY23 Defense Policy Bill that Includes $37B Amendment
A number of research and development projects are supported by the amendment, including a $665 million plus-up for biomanufacturing and biotechnology, $325 million for test and evaluation infrastructure, $200 million for quantum computing, and $200 million for 5G and FutureG communications technology.

FACT SHEET: President Biden Announces Two Presidential Directives Advancing Quantum Technologies
Research shows that at some point in the not-too-distant future, when quantum computers reach a sufficient size and level of sophistication, they will be capable of breaking much of the cryptography that currently secures our digital communications on the Internet.

National Security Memorandum on Promoting United States Leadership in Quantum Computing While Mitigating Risks to Vulnerable Cryptographic Systems
It directs specific actions for agencies to take as the United States begins the multi-year process of migrating vulnerable computer systems to quantum-resistant cryptography.

Executive Order on Enhancing the National Quantum Initiative Advisory Committee
To ensure that the NQI Program and the Nation are informed by evidence, data, and perspectives from a diverse group of experts and stakeholders, the National Quantum Initiative Advisory Committee (Committee) is hereby established.

DOE Announces $40 Million to Provide Research Training Opportunities for Historically Underrepresented Groups
The Advanced Scientific Computing Research (ASCR) FOA will broaden the quantum computing and networking workforce by creating new research and classroom-based training opportunities for students, postdoctoral researchers, and faculty from underrepresented groups and at historically underrepresented institutions such as non-R1 institutions and/or MSIs.

Singapore ups investment in quantum computing to stay ahead of security threats
The Singapore government on Tuesday announced plans to set aside SG$23.5 million (17.09 million) to support three national platforms, parked under its Quantum Engineering Programme (QEP), for up to 3.5 years.

White House cyber official: U.S. beating China in race to quantum supremacy
The United States is in a “generally favorable position vis-à-vis China” in the race to win on quantum computing, according to the National Security Council’s Director for Cyber and Emerging Tech Policy Jonah Force Hill.

Special Operations Command trying to prepare for quantum computing threat
"Here's a really interesting aspect of this that we're looking at today because we know in a few years this is going to become really important — by some accounts, we're less than eight years away from quantum cryptography being able to break the non-quantum cryptography that we have today ... We need an answer for that," he said.

NSA involvement in encryption project raises suspicions
"Back doors are only possible when you are obscuring things," said Vince Berk, the chief revenue and strategy officer at Quantum Xchange, a cybersecurity vendor focused on encryption. "Crypto algorithms are just that — algorithms. [Encryption] implementations can be made by anyone, and that is usually when the back doors go on."

Western democracies craft alliance on quantum technology
The countries involved want to better understand and coordinate each other's national quantum initiatives, which have proliferated in recent years as governments have cottoned on to the potential of the field.

NSA Says 'No Backdoor' for Spies in New US Encryption Scheme
The NSA already has classified quantum-resistant algorithms of its own that it developed over many years, said Joyce. But it didn't enter any of its own in the contest. The agency's mathematicians, however, worked with NIST to support the process, trying to crack the algorithms in order to test their merit.

Japan bans exports of quantum computers to Russia in latest sanctions
Japan will put the ban in place May 20 to prevent the items from being diverted for military use, in line with an agreement with its Group of Seven partners to prohibit shipments of cutting-edge products to Russia.

New error mitigation approach helps quantum computers level up
The novel error mitigation approach will allow researchers to run longer, more realistic simulations and still obtain reliable results. This will broaden the potential impact of upcoming quantum computers on scientific discovery.

Washington's new crush on quantum computing
A bipartisan House bill introduced Monday would boost federal support for quantum-resistant encryption. And a whole slew of provisions related to quantum sciences are more likely than this latest bill to become law this year — and could see action as soon as Congress returns from recess.

Exascale in China? 40 Million Cores Used for Many-Body Quantum Simulation
"This development adds credibility to the notion that China may have deliberately not reported exascale Linpack results for the November 2021 Top500 list in order to avoid attracting more U.S. Government restrictions"

More International Quantum Partnerships Likely As U.S. Stakes Claim In Field
Announcing a new partnership with Sweden on Wednesday, the U.S. has now entered several bilateral agreements specifically focused on quantum tech development with various ally countries, including Japan, Australia, Finland and the U.K.

Quantum secure communication breakthrough for China scientists
His team said they have set a new distance record, sending information securely over 100km (62 miles). While transmission speeds were slow – at just 0.54 bits per second – it is a significant jump from Long's 2020 record of 18.5km

Outgunning The US, China Looks At Gaining Unassailable Lead In Quantum Tech With New Helium Cooling System
This new cooling device makes use of Helium-4, another helium isotope that is used as a gas for party balloons. Helium-4 is much more abundant than Helium-3 but is less effective as a coolant in extreme conditions.

How is China Educating a Quantum Workforce?
Thirty-seven new majors were included in the catalogue of undergraduate majors in ordinary colleges and universities of which quantum information science is one. Several universities started their quantum information undergraduate coursework.

NATO and White House recognize post-quantum threats and prepare for Y2Q
The NATO Cyber Security Center (NCSC) announced that it had tested a post-quantum VPN provider by U.K.-based quantum computing provider Post-Quantum, to secure its communication flows.

Top Government's Budget for Quantum Computing in 2022
The governments have started allocating million dollars budgets for investing in quantum computing for 2021-2025. Let's know which country is pacing forward to be at the top of Quantum computing. China, USA, France, Japan, South Korea, India, Germany

DARPA Announces Quantum Computing Program
US2QC aims to determine if an underexplored approach to quantum computing is capable of achieving utility-scale operation much faster than conventional predictions. "If a company or an organization thinks they can make a truly useful, really big, fault-tolerant quantum computer, we want to have a conversation with them," Altepeter said.

Biden's cybersecurity order opens our post-quantum era
The White House has released a National Security Memorandum that, for the first time, focuses our national security concerns on the future threat of large-scale quantum computers to encrypted data, which means everything from government records and classified data to credit cards and banking transactions.

Quantum Tech Still Too Young to Warrant Export Controls, Defense Advisers Warn
Sponsored from within the Office of the Undersecretary of Defense for Research and Engineering, the report provides a more nuanced review of what's often simply described as a competition between China and the U.S. It also points to roles for various specific agencies as the issue advances.

India to invest $1bn in quantum computing
It is also planning to develop a quantum computer with about 50 qubits by 2026, joining a growing number of countries such as Australia and Israel that are looking to drive broader adoption of the nascent technology.

China releases new quantum computing software
China has released a new quantum computing programming software named "isQ-Core" and deployed it to the country's superconducting quantum hardware platform.

What Europe's $48 billion chips plan could do for quantum computing
The European Chips Act, which still has to be approved by EU member states and lawmakers, would temporarily re-write strict rules that regulate when and how individual countries are allowed to subsidize industries within their borders.

Pronouncements and Commentary

Keysight Introduces a New Quantum Control System for Use in Quantum Processors

Keysight has developed a new modular Quantum Control System that provides high levels of signal accuracy using a technology called Direct Digital Synthesis.

IonQ and GE Research Demonstrate High Potential of Quantum Computing for Risk Aggregation

IonQ and GE are able to use a large set of data to model predictability associated with future risk across up to four variables using their quantum computers.

IDC Perspective on Integration of Quantum Computing and HPC

IDC expects investments in the quantum computing market will reach nearly $16.4 billion by the end of 2027.

Announcing the AWS Center for Quantum Networking

They have evolved from delicate laboratory systems accessible to only a few research institutions to increasingly reliable and powerful commercial machines available to researchers, developers, and even quantum enthusiasts worldwide via cloud services like Amazon Braket.

The Road to the Hybrid Quantum-HPC Data Center Starts Here

As quantum systems evolve, the next big leap is a move to hybrid systems: quantum and classical computers that work together. Researchers share a vision of systems-level quantum processors, or QPUs, that act as a new and powerful class of accelerators.

Diamond-based quantum computer paired with supercomputers for first time

That marks the first time a quantum computer has been integrated directly into a rack alongside a traditional supercomputer – in this case, Pawsey's new HPE Cray Ex supercomputer, Setonix.

Microsoft aims to win the race to build a new kind of computer. So does Amazon

The companies are riding a swell of interest that could grow to $9.1 billion in revenue by 2030, according to Tractica, a market intelligence firm that studies new technologies and how humans interact with tech advancements.

QED-C® announces four projects designed to advance cryogenics for Quantum Information Science and Technology

"This program will help accelerate the pace of U.S. innovation and commercialization in the field of quantum," said Celia Merzbacher, QED-C executive director. "QED-C plans for additional research opportunities for consortium members in the coming year in an effort to remove further barriers and enable advances in quantum technology and applications."

Quantinuum Introduces InQuanto Quantum Chemistry Platform
It was developed and deployed by Quantinuum's quantum chemistry team to support collaborations with partners such as BMW, JSR, Nippon Steel Corporation, and TotalEnergies, to explore quantum computing use-cases specific to their industry.

Is quantum computing headed for a financial reckoning?
The challenges faced by quantum computing firms that have gone public via SPAC deals are happening amid an environment in which billions of dollars have been invested in quantum start-ups in recent years–as much as $3.2 billion last year alone, $1 billion of which came in the final quarter of the year.

IBM Unveils New Roadmap to Practical Quantum Computing Era; Plans to Deliver 4,000+ Qubit System
This roadmap details plans for new modular architectures and networking that will allow IBM quantum systems to have larger qubit-counts – up to hundreds of thousands of qubits.

Turning A Million-Qubit Quantum Computing Dream Into Reality
In a peer-reviewed research paper published earlier this year, Intel says it successfully fabricated more than 10,000 arrays, each with three to 55 quantum dots, on a 300-millimeter wafer with a yield higher than 95 percent.

AWS now offers a 'quantum-powered' random number generation service
Amazon Web Services (AWS) Marketplace now offers a quantum computing-based random number generation service, developed by the Australian National University's Quantum Numbers project (AQN).

Keysight Signs MOU with Singapore's QEP to Accelerate Quantum R&D
QEP and Keysight will closely cooperate in the development of quantum instrument packages, as well as the technologies that enable quantum systems to be scalable and deployable.

Combining the Advantages of Classical Computing with Quantum Computing to Tackle Optimization Problems
Over the next two years, the team plans to use several hundred quantum bits (qubits) made of trapped ions to put the unique capabilities of quantum computing systems to work on these challenges.

Intel and QuTech Collaborate to Produce Silicon Qubits at Scale
The result is a process that can fabricate more than 10,000 arrays with several silicon-spin qubits on a single wafer with greater than 95% yield.

IonQ and Hyundai Motor Expand Partnership to Use Quantum Computing for Object Detection
IonQ and Hyundai will look to develop quantum techniques for the broad task of 3D object detection, expanding the current work on recognizing road signs to include other objects like pedestrians or cyclists.

IBM Announces the z16 Mainframe

Building on IBM technologies such as Pervasive Encryption and Confidential Computing, IBM z16 takes cyber resiliency further by protecting data against future threats that could evolve with advances in quantum computing.

Quantinuum Announces Quantum Volume 4096 Achievement

Quantum computing development company Quantinuum announced that the System Model H1-2 doubled its performance "to become the first commercial quantum computer to pass Quantum Volume 4096, a benchmark introduced by IBM in 2019 to measure the overall capability and performance of quantum computers."

IBM's new Qiskit primitives make it easier to develop algorithms for quantum computers

Dubbed "Sampler" and "Estimator," the two new primitives essentially containerize many of the necessary steps in order to streamline the quantum computing stack for devs.

Build your own quantum computer with Google's latest 'simulator'

Created in partnership with Double-speak games, it's a "playful journey to building a quantum computer, one qubit at a time," Google said. It also hopes the game, and World Quantum Day, will help generate some interest in the field.

IonQ Announces Full Year 2021 Financial Results and Provides Business Update

IonQ expects revenue for 2022 to be 5x IonQ's 2021 topline. For the full year 2022, IonQ expects revenue to be between $10.2 million and $10.7 million, with between $1.8 million and $2.0 million for the first quarter.

Chicago Quantum Exchange Publishes 2022 Annual Report

These successes are part of the CQE's annual report, published this month, which highlights the many accomplishments of its members and partners.

IBM invests in Honeywell's Quantinuum

Quantinuum this week announced an agreement with IBM to expand the IBM Quantum Hub with Cambridge Quantum Computing Limited, providing clients with access to IBM's quantum computing systems.

2022:

15 Aug: Workshop on Scalable Quantum Control

19–21 Aug: Workshop for Quantum Repeaters and Networks

21–25 Aug: SPIE Quantum Communication and Quantum Imaging Conference, San Diego

24–28 Aug: Superconducting Qubits and Algorithms Conference, Helsinki, Finland.

29 Aug–2 Sep: Conference on Quantum Information and Quantum Control IX

29–31 Aug: Solvay Workshop on Quantum Simulation 2021, Brussels

4–9 Sep: Frontiers of Quantum Information Science, Vienna, Austria

5–9 Sep: Conference on Spin-Based Quantum Information Processing

18 Sep: Quantum Science and Engineering Education Conference

18–23 Sep: IEEE Quantum Week 2022, Denver, Colorado

18–23 Sep: IEEE Intl. Conf. on Quantum Computing and Engineering, Denver, Colorado

13–14 Oct: Workshop on Quantum Computing and Operations Research

23–28 Oct: Applied Superconductivity Conference

31 Oct–4 Nov: Single Photon Workshop 2022, Seoul, South Korea

8–11 Nov: Quantum Techniques in Machine Learning (QTML 2022), Naples, Italy

13 Nov: International Workshop on Quantum Computing Software

2023:

6–10 Feb: Quantum Information Processing (QIP 2023), Ghent, Belgium

10 Apr–5 May: Quantum Computing Methods for High Energy Physics, Munich, Germany